



124
794
THS



23074506

LIBRARY
Michigan State
University

This is to certify that the

thesis entitled

A Model for the Determination of the
Loads Carried by the Internal Structures of
the Lower Limb: A Biomechanical Application
of Optimization Theory

presented by

Lisa Margaret Schutte

has been accepted towards fulfillment
of the requirements for

M.S. degree in Mechanics

Major professor

Date August 31, 1988

PLACE IN RETURN BOX to remove this checkout from your record.
TO AVOID FINES return on or before date due.

DATE DUE	DATE DUE	DATE DUE
OCT 30 2004	_____	_____
_____	_____	_____
_____	_____	_____
_____	_____	_____
_____	_____	_____
_____	_____	_____
_____	_____	_____

MSU Is An Affirmative Action/Equal Opportunity Institution

A MODEL FOR THE DETERMINATION OF THE LOADS CARRIED BY THE
INTERNAL STRUCTURES OF THE LOWER LIMB: A BIOMECHANICAL
APPLICATION OF OPTIMIZATION THEORY

By

Lisa Margaret Schutte

A THESIS

Submitted to
Michigan State University
in partial fulfillment of the requirements
for the degree of

MASTER OF SCIENCE

Department of Metallurgy, Mechanics and Materials Science

1988

ABSTRACT

A MODEL FOR THE DETERMINATION OF THE LOADS CARRIED BY THE INTERNAL STRUCTURES OF THE LOWER LIMB: A BIOMECHANICAL APPLICATION OF OPTIMIZATION THEORY

By

Lisa Margaret Schutte

This research investigated the loads carried by the various internal structures of the lower limb during physical activity. The extent to which these predicted loads change when different theoretical models are applied was also determined.

A nonlinear static optimization problem, minimizing the summation of the muscle stresses cubed, was formulated in order to solve the redundant biomechanical problem for the stance phase of running. A three-dimensional model of the lower limb was developed. Several variations to this model, accounting for the ligamentous contribution and the point of bony contact at the knee in different ways, were investigated. The ligamentous contribution to the total joint moments and thus its effect on the predicted muscle forces, was found to be quite small. Distinct differences in the patterns of muscle activity were seen for each of the model variations.

ACKNOWLEDGMENTS

The author wishes to express her appreciation to the following people for making the completion of her Master of Science degree possible:

To Dr. Robert Wm. Soutas-Little, her major professor, for his warm friendship, encouragement and guidance over the last two years.

To the National Science Foundation and Brooks Shoe, Incorporated, for their generous support of her education and research.

To Julia E. Suber, for her support, encouragement and most of all her warm and loving friendship.

To Robert Johnson, Robert Streight and Richard Cohn, for the warmth and laughter of their friendship which helped to make life bearable during the long task of writing this manuscript.

To her sister, Tracie, the Physical Therapist, for helping to make sense of the clinical implications of this research.

To her family, for their encouragement and understanding in her academic pursuits and for their constant love and support.

TABLE OF CONTENTS

	Page
LIST OF FIGURES.....	v
LIST OF TABLES.....	vii
LIST OF NOMENCLATURE.....	viii
Sections	
I. INTRODUCTION.....	1
II. SURVEY OF LITERATURE.....	5
III. ANATOMICAL MODEL.....	21
IV. ANALYTICAL METHODS.....	44
V. RESULTS AND DISCUSSION.....	59
VI. CONCLUSION.....	80
APPENDIX - GENERALIZED REDUCED GRADIENT METHOD.....	83
BIBLIOGRAPHY.....	89

LIST OF FIGURES

Figure	Page
1. LOCAL COORDINATE SYSTEMS FOR THE DESCRIPTION OF MUSCLE ORIGINS AND INSERTIONS.....	24
2. COMPARISON OF MUSCLE MODEL TO ACTUAL MUSCULATURE OF THE LOWER LIMB.....	27
3. ASSUMED RELATIONSHIP BETWEEN TIBIAL TUBEROSITY AND CENTER OF TIBIAL PLATEAU.....	30
4. TWO-DIMENSIONAL JOINT SURFACES.....	37
5. ANTERIOR-POSTERIOR COORDINATE OF CONTACT POINT ON TIBIAL SURFACE.....	40
6. EXTERNAL JOINT FORCES AND MOMENTS.....	45
7. FREE BODY DIAGRAM OF FORCES ACTING ON THE LOWER LIMB.....	49
8. MOMENT RELATIONSHIP.....	52
9. ANKLE MOMENTS.....	60
10. KNEE ANGLES.....	62
11. HIP ANGLES.....	62
12. LIGAMENT EXTENSION RATIOS WITH RESPECT TO FLEXION ANGLE.....	63
13. LIGAMENT EXTENSION RATIOS, DURING STANCE PHASE OF GAIT.....	65
14. PATTERN OF MUSCLE ACTIVITY, LONG HEAD OF BICEPS FEMORIS.....	72
15. PATTERN OF MUSCLE ACTIVITY, RECTUS FEMORIS.....	72
16. PATTERN OF MUSCLE ACTIVITY, SEMIMEMBRANOSUS.....	73
17. PATTERN OF MUSCLE ACTIVITY, SEMITENDINOSUS.....	73

18.	PATTERN OF MUSCLE ACTIVITY, TENSOR FASCIAE LATAE...	74
19.	PATTERN OF MUSCLE ACTIVITY, MEDIAL GASTROCNEMIUS...	74
20.	PATTERN OF MUSCLE ACTIVITY, LATERAL GASTROCNEMIUS..	75
21.	PATTERN OF MUSCLE ACTIVITY, SHORT HEAD OF BICEPS FEMORIS.....	75
22.	PATTERN OF MUSCLE ACTIVITY, VASTUS INTERMEDIUS.....	76
23.	PATTERN OF MUSCLE ACTIVITY, VASTUS LATERALIUS.....	76
24.	PATTERN OF MUSCLE ACTIVITY, VASTUS MEDIALIUS.....	77
25.	PATTERN OF MUSCLE ACTIVITY, GLUTEUS MAXIMUS 1.....	77
26.	PATTERN OF MUSCLE ACTIVITY, GLUTEUS MEDIUS 1.....	78
27.	PATTERN OF MUSCLE ACTIVITY, ILIACUS.....	78

LIST OF TABLES

Table	Page
1. SCALED LOCAL COORDINATES OF MUSCLE ATTACHMENTS (BRAND'S DATA).....	26
2. MUSCLE SCALE FACTORS.....	28
3. PHYSIOLOGICAL CROSS-SECTIONAL AREA OF INDIVIDUAL MUSCLES.....	33
4. LOCAL COORDINATES OF LIGAMENT ATTACHMENTS.....	35
5. LIGAMENT PARAMETERS.....	36
6. ACTUAL SUBJECT SCALE FACTORS.....	61
7. RESULTS FOR ALL SIX CASES, 0.12 SECONDS AFTER HEEL STRIKE.....	67
8. RESULTS, WITH AND WITHOUT LIGAMENTS, 0.22 SECONDS AFTER HEEL STRIKE.....	69

LIST OF NOMENCLATURE

α	Angular acceleration of the body segment.
θ	Flexion - extension angle.
ϕ	Abduction - Adduction angle.
γ	Internal - external rotation.
$a_{cm}^{(f)}, a_{cm}^{(s)}, a_{cm}^{(t)}$	Acceleration of the center of mass of the segment.
A_i	Physiological Cross-Sectional Area of the i th muscle.
f_i	The force in the i th muscle.
F_1, F_2, F_3, F_4, F_5	The sum of the forces in each of the categories of muscles. The categories are determined by the body segments the muscles act between.
F_{ca}, F_{ck}, F_{ch}	The joint contact forces at the ankle, knee and hip.
F_{csh}	The shear component of the knee contact force.
F_{LA}, F_{Lk}, F_{Lh}	The total ligament forces at the ankle, knee and hip.
F_{Li}	The force in the individual ligaments at the knee.
F_{PL}	The force in the patellar tendon.
F_{PAT}	The force exerted on the femur by the Patella.
F_{Q1}, F_{Q2}	The sum of the one joint muscles and the two joint muscles respectively in the quadriceps group.

\hat{n}

The unit normal to the knee joint surface.

$p_{cm}(f), p_{cm}(s), p_{cm}(t)$

A vector from the proximal joint center to the center of mass of the segment.

$r_i(f), r_i(s), r_i(t)$

A vector from the proximal joint center to a point along the line of action of an applied force, i .

$R(f), R(s), R(t)$

A vector from the proximal joint center to the distal joint center of the segment.

INTRODUCTION

For most physical activities the lower limbs are the link between external loading and the rest of the human body. The forces that the ground exerts on the feet are transmitted through the legs, affecting the knee, hip and back. Abnormal gait can thus be related to physical problems or pain in other portions of the body. The legs, as well as the rest of the body, are made up of ligaments, muscles, cartilage, and bone, functioning together in order to support the body and produce desired motions. Active muscle function is accompanied by passive function of the joint ligaments and articular surfaces. Even the simplest of human motions is characterized by patterns of agonistic, antagonistic and synergistic muscle activity.

An understanding of the distribution of internal loads and the role the the various elements play is desirable for many reasons. Information as to how ligaments and muscles function normally and how their role changes as a consequence of intervention can be valuable to physicians and surgeons. Injuries due to ligament tears and muscle strain are common in many sports activities as well as in everyday living. This is especially true for the knee joint, which due to its exposed position and the large forces that

it is subjected to, is one of the most frequently injured joints in the body. Information from knee research can serve to determine possible sources of injury in various activities, establish extremes to avoid, and suggest possible means of prevention.

The human body is a complex and often redundant mechanical system, and the lower limb is no exception. There are thus many difficulties associated with understanding and measuring how the various elements function together. The important structures are generally inaccessible, making direct in-vivo measurements difficult and in-vitro testing does not always accurately imitate function in the living system. Non-invasive techniques such as EMG can give a measure of muscle activity but this information is basically qualitative; telling which muscles are active but not how much force they are producing. Three-dimensional kinematics can be measured using stereocinematography or six degree of freedom goniometers but soft tissue motion can be a major source of error. Motions out of the sagittal plane tend to be small, making these inaccuracies even more significant.

A high degree of variability exists between individuals both in anthropometric characteristics and in the specific way various motions are executed. Differences in height, build ect. result in variations in the moments arms and lines of action associated with muscle and ligament forces. Basic mechanical properties of human tissues are also

subject to variations as a result of age, health and physical condition.

Even solving mathematically for the loads carried by the various structures is a source of difficulty due to the redundant nature to the problem. The redundancy serves to increase the flexibility of the system, making a wide variety of motion possible. The number of ligaments and muscles crossing any one joint is generally greater than the number of equations that can be written relating these forces. The system is thus underdetermined and no unique solution exists.

Load sharing among the structures of the musculoskeletal system has been studied by a variety of methods. The redundant nature of the problem has been handled by simplification to a determinate problem as well as by use of static and dynamic optimization techniques. More recently, random stochastic criteria have been applied. Among the passive structures finite element methods have been applied as well as geometric compatibility relationships. For the most part the active elements (muscles) and the passive elements (ligaments) have either been treated separately or one emphasized while the other is treated as a lumped parameter. Since the load transmitted across any joint is carried by a combination of both types of structures it seems reasonable that the load carried by one would not be independent of the load carried by the

other, but rather that a certain degree of interdependence would be displayed.

The purpose of this research was to develop a model of the internal structures, both passive and active, of the lower limb, especially those crossing the knee joint, in order to study this interdependence. This involved determining the locations of the attachments and lines of actions of the various muscles and ligaments. Representations of the joint surfaces were also developed in order to describe the point of joint contact and thus the relative positions of the bony structures to which the muscles and ligaments attach. Geometric compatibility relationships and static optimization techniques were applied in order to quantify the load carried by the individual structures. The effect of various alternative methods of treating ligament contributions to the muscle optimization problem were also investigated.

SURVEY OF LITERATURE

The human musculoskeletal system can be treated as a system of rigid articulating links acted on by known and unknown forces. Quantities such as ground reaction forces, weight of the segments or externally applied forces are usually measurable or in some way derivable. Other forces such as those associated with the ligaments and muscles acting on the system are not so easy to quantify. These internal forces are difficult to measure directly on living subjects, and the number of these components acting on any one segment generally exceeds the maximum number of equilibrium equations or equations of motion that can be written for the segment. An underdetermined system of equations, where the number of unknown values exceeds the number of equations, generally results.

The usual method in engineering applications for treating statically indeterminate problems is to complement the equilibrium equations with relationships involving deformations. By considering the geometry of the problem, deformation relationships can be found and from known force-deformation or constitutive equations the load carried by the elements in the structure can be calculated. This idea can be applied to the ligamentous structures in the body but

not to the muscles. Because of the unique contractile mechanisms involved, the muscles present a more difficult challenge. Unique relationships between deformation and load cannot be determined. In the case of isometric contractions, for example, a significant force can be produced by a muscle which undergoes no change in length.

Since the Weber brothers in 1836 claimed that during the swing phase of gait, muscular control was not necessary and that the motion of the leg occurred much like a pendulum (40), there has been interest in the role that these internal structures play in gait as well as in other activities. Early gait work such as that of Elftman(1939) and Bresler and Frankel(1950) (14,7), as well as many more contemporary studies, has focused mainly on determining the total forces and moments transmitted across each joint. These forces are carried by the individual muscles and ligaments crossing the joint and the contact force between the articulating surfaces.

Early attempts to determine the distribution of the total joint forces among the various components involved simplification of the underdetermined problem to one that was determinate. Morrison in 1968 used a three-dimensional model to predict how the external load transmitted across the knee was shared by the internal structures (28). He condensed these structures into three muscle groups—quadriceps femoris, hamstrings and gastrocnemius, and four ligaments—two cruciates and two collaterals. He made

further assumptions based on experimental data such as EMG measurements to eliminate "inactive" components and further reduce the problem to one with six equations and six unknowns.

The intuitively appealing idea that the body uses no more total muscular force than is necessary and sufficient to maintain a posture or perform a motion was first proposed as the "Principal of Minimal Total Muscular Force" by MacConaill in 1967 (25). This idea suggested the application of optimization theory where some criterion--referred to as the cost function or objective function--subjected to equality constraints in the form of the equilibrium equations, is minimized or maximized to solve the indeterminate problem of muscle loadings. Several investigators since have applied MacConaill's postulate to predict a possible distribution of muscle forces by minimizing the function:

$$U = \sum F_i$$

where: F_i = The individual muscle forces.

Barbanel in 1972 applied this cost function to the loading of the temporal mandibular joint (3), and Seireg and Arviker in 1973 to the muscles of the lower extremity during various static postures (35). Penrod in 1974 and Yeo in 1976 applied it to the wrist and elbow, respectively, while Hardt(1978), Pedotti et al(1978) and Patriarco et al(1981) applied this criterion to level walking (33, 39, 19, 32, 29).

Penrod also proposed an objective function to minimize the total muscle stress (33). This criterion takes into account the relative size of each of the individual muscles and is of the form:

$$U = \sum F_i / A_i$$

where A_i is the physiological cross-sectional area of the muscle, defined to be the volume of the muscle divided by its length.

Other linear criteria that have been applied include weighted sums to muscle and ligament moments and forces by Seireg and Arviker (34) and minimization of the maximum muscle stress proposed by An in 1984 (1). This later criterion is based on the idea that since each muscle bundle has its own energy storage capacity and blood supply, individual muscle effort rather than the overall system effort is important. The disadvantage of this criterion is that if more than one moment equilibrium equation appears as an equality constraint, a unique solution is not assured. Bean, Chaffin and Schultz in 1988 improved on this criterion in reference to the lower back (4). They proposed a two-fold linear optimization algorithm where the maximum muscle stress was minimized, and then using that maximum value as an inequality constraint, a second problem minimizing spinal compression was solved.

Unfortunately, the linear criteria, in general, do not always produce results which are physiologically consistent. When no additional constraints other than equality

constraints resulting from equilibrium or motion equations are applied, minimizing the total muscular force becomes purely a geometric criterion, favoring the muscle with the longest moment arm. When it is applied to a single joint planar model, only a single muscle will be predicted to be active. Since muscles are known to display synergistic as well as antagonistic activity, this is not a reasonable result. In order to predict a wider distribution of muscle loading, the formulation of additional constraints, such as upper limits on the force or stress in any one muscle, were advocated by many investigators, including Penrod, Yeo, Pedotti and Hardt (33, 39, 32, 19). This increases the number of active muscles from the unconstrained case, but the total number of muscles involved is still limited. An additional muscle can become active only when one muscle is saturated. Since the upper limits on the muscle capabilities are estimated and not known exactly, the selected solution is somewhat arbitrary. Crowninshield in 1978 demonstrated the extent to which the solution could be affected by the choice of this upper limit (9).

Patriarco formulated an additional equality constraint to enforce synergism between two muscles by assuming equal stresses (29). A sufficient number of these enforced synergisms, though, could make the problem deterministic. At this extreme the problem is not so different from that solved by Morrison.

The use of nonlinear objectives is, in general, more successful in predicting a greater number of active muscles and thus synergistic behavior. Unfortunately, obtaining a solution to a nonlinear problem is more difficult, as convergence to a global optimum is not always assured.

Nonlinear objective functions such as:

$$U = \sum (F_i)^2$$

and
$$U = \sum (F_i/F_{i\max})^2$$

were first proposed by Pedotti in 1978 as criteria which would use the muscle most efficiently by penalizing large individual muscle forces (32). These criteria were an attempt to find a solution where realistic amounts of synergistic behavior would be displayed. There was little real physiological basis behind them. Crowninshield and Brand later proposed a nonlinear cost function which did have physiologically supported origins (10). It was related to maximizing the endurance time of an activity and was of the form:

$$U = \sum (F_i/A_i)^{n_i}$$

where the parameter n_i is related to the percentage of slow twitch fibers in the i th muscle. Since a reasonable value for n is approximately three for most muscles, this endurance-based criterion reduced to one of minimizing the sum of the cubes of the muscle stresses. The fact that this criterion predicts a greater number of active muscles is consistent with the idea that the endurance is maximized. Low individual muscle stresses are achieved by predicting

activity in a large number of muscles. Since individual muscle stresses are low, their ability to display prolonged contractions is increased. Endurance criteria of this type are applicable for activities that involve sustained or repetitive muscular contraction such as sitting, standing or walking. These contractions are fatiguing. The required mechanical output to produce actions of this sort can only be maintained for a specific period of time. It is assumed that the neuromuscular system anticipates this by selecting a load sharing between muscles such that the endurance time is maximized and the muscular fatigue minimized. This concept may be less useful for activities involving quick, nonrepetitive contractions. The convex nature of this problem, with a continuous convex objective function and linear constraints, assures that the only minimum is the global minimum.

A similar endurance-based criterion was proposed by Dul et al in 1984 (13). Dul's criterion was to maximize the minimum of:

$$T_i = a_i (F_i \times 100 / F_{i\max})^{n_i}$$

where a_i and n_i are again related to the percentage of slow twitch muscle fibers.

All of the above-mentioned optimization problems can be classified into the category known as static optimization. All of these either involve static situations such as standing, lifting etc., where motions are insignificant and static equilibrium equations can be applied, or dynamic

situations such as gait which are treated in a quasi-static manner. In the latter case the optimization problem is solved repeatedly at set time intervals in the motion with dynamic equilibrium equations based on D'Alembert's Principle, applied as time-varying equality constraints. No excitation or contraction dynamics of the muscles are included in these models. For the dynamics problem this type of analysis has some disadvantages. For most optimization criteria, the predicted muscle forces depend mainly on the geometry of the problem and the applied external forces. With the exception of the $(F_i/F_{i\max})^2$ criterion advocated by Pedotti and the endurance criterion proposed by Dul, which both incorporated the idea that muscle action depends on the muscle velocity ($F_{i\max}$ is proportional to the velocity), the current state of the muscle is not taken into account. This ignores the reasonable idea that it would be more effective to continue to stimulate a muscle which is already active than to turn it off and stimulate another. The muscle action at any instant is assumed to be independent of actions at all other times. The problems associated with this are most obvious with linear optimization criteria which often display large fluctuations in the results.

Dynamic optimization techniques which involve aspects of optimal control theory have been proposed by several investigators including Davey(1987) and Zajac(1984) (12, 42). In general, these problems differ from static

optimization in that more basic models of muscle excitation and contraction are involved. Static methods look at the forces produced, not how they are produced. The calculations necessary to solve dynamic problems become very complex, often limiting the detail of the model that can be used. Davey's model for gait, for example, was two-dimensional and only considered nine muscles in the lower extremity.

An alternative to either static or dynamic optimization methods was proposed in 1988 by Mikosz, Andriacchi and Andersson (26). They applied a three-dimensional stochastic mathematical muscle model of the knee joint in order to determine the muscular force around the joint. Their computational technique involves selection of muscle forces on a random basis within physiological constraints. The idea behind this is that the body randomly chooses a solution from among the infinite number of physiologically reasonable choices available in the redundant system. This is in contrast to the assumption made by applying optimization techniques--that the body makes the choice based on some set logical criterion and that the same pattern of muscle activity will always be used to produce a given action.

The role of the ligaments in the various optimization solutions has, in general, been poorly defined. Some investigators, such as Dul and Barbanel, chose to ignore their effect completely, concentrating instead on the muscle

activity (13, 3). Others have included the ligaments in a more general way, especially at the knee. Crowninshield and Brand, Seireg et al, Hardt and Pedotti all treated the knee as a simple hinge joint (10, 35, 19, 32). Although they did not calculate ligament forces, they did consider the motion out of the sagittal plane to be constrained by the ligaments. Crowninshield and Brand modeled this by requiring the muscles, which were described in three dimensions, to satisfy only the flexion-extension component of the moment at the knee (10).

Patriarco took another route by increasing the tolerances on the equilibrium equations (29). Thus the contribution of the ligaments to these equations, though not explicitly included, could be considered in the optimization. Others such as Seireg et al and Gracovtsky included ligaments in their objective function (34,16). Gracovetsky did not mathematically distinguish between ligaments and muscles, treating them both as unknown analysis variables to be determined by optimization.

The knee is a very complex joint. The Weber brothers were the first to notice that knee flexion occurs by a combination of rolling and sliding between the tibia and femur and that flexion does not occur in a single plane but is accompanied by axial rotation of the tibia (40). The simple hinge joint idea applied in many of the optimization methods thus does not adequately describe this complex motion. More complex models of the knee which consider the

geometry and ligamentous structure of the knee have been equally lacking in their treatment of muscle activity. As pointed out by Hefzy and Grood in a 1987 review of knee models, the complexity of this joint is reflected in the lack of a comprehensive model (20). Although much theoretical and experimental work has been done on the knee, there is still much that remains to be explored. Even a two-dimensional model that includes both patello-femoral and tibio-femoral joints does not yet exist, and three-dimensional models have been limited to the quasi-static case, and thus cannot adequately predict the effects of dynamic inertial loads. The experimental work in this area has often led to conflicting or at least confusing results, making validation of the various models difficult.

The kinematics of the knee joint have principally been described by one of two methods: a screw axis formulation or Euler angles. Various Euler angle descriptions have been used by investigators to describe the relative rotational motions between the tibia and femur. Among these are the joint coordinate system advocated in 1983 by Grood and Suntay (18). This system prescribed rotations about anatomically significant axes. It also allowed for the inclusion of translatory movement, giving the model six degrees of freedom.

Early mathematical models to describe the kinematics of the knee include Strasser's 1917 four-bar linkage system (37). This modeled four principal components of the joint,

namely the tibia, femur and two cruciate ligaments, as an interconnected four-bar linkage. This simple model did account for many basic properties of knee movement, including the posterior movement of the tibia-femur contact point.

Models to determine the forces in the passive structures of the knee under equilibrium as well as dynamic conditions have generally followed the basic concept that as bones are displaced, ligaments are stretched and forces develop. While, in theory, load can be calculated if the deformations are known, the relationship between these two quantities for the ligaments is not completely understood. The relationship is a nonlinear one, complicated by extreme differences between individuals, difficulty in accurately determining initial lengths of the ligaments and their attachment points and questions as to the validity of in-vitro tests. Despite these limitations, several investigators have developed comprehensive models of the passive knee structures in order to theoretically predict this loading. Several of these are described below.

Crowninshield, Pope and Johnson in their 1976 publication developed a model which included thirteen ligamentous components, each treated as a nonlinear spring acting in a straight line between the attachment points (11). Portions of the more complex structures were treated separately, such as the posterior and anterior portions to the anterior cruciate. This allowed for the conflicting

motions seen in these structures and provided a way to include the twisting motions to these elements. Coordinates of the attachment points of these ligaments in an unflexed position were determined from cadaver knees. New coordinates at given flexion angles were then calculated. Other displacements such as internal-external rotations and joint translation were given as a function to flexion angle based on quantities available in the experimental literature of that time. Thus the external forces acting on the joint were not included in the model at all. Once the new coordinates were known, the difference between the flexed and unflexed ligament lengths could be easily computed. Assuming a nonlinear relationship between the strain and the tensile force in each ligament of the form:

$$F = 750 A \left(\frac{l - l_0}{l_0} \right)^2$$

where: A = the cross-sectional area of the ligament in mm²

l_0 = the slack length of the ligament, assumed to be 95% of the maximum length of the ligament calculated during normal flexion.

These investigators were able to calculate a force associated with each ligament. By combining the results for all ligaments, relative joint stiffnesses were calculated.

Grood and Hefzy in 1982, using a physical model similar to Crowninshield's, derived an expression for the nonlinear coupled stiffness characteristics of the knee at a given joint position (17). They applied a method of matrix

structural analysis in order to do this, calculating a 36 element stiffness matrix of the form:

$$[S] = \begin{bmatrix} \partial F_i / \partial x_j & \partial F_i / \partial \theta_j \\ \partial M_i / \partial x_j & \partial M_i / \partial \theta_j \end{bmatrix} \quad i, j = 1, 2, 3$$

Their model did not calculate individual tensile forces in the ligaments explicitly but instead related the total joint loads resulting from the ligamentous structures with the joint displacements. In a second 1983 paper, Hefzy and Grood expanded their model to take into account geometric nonlinearities caused by ligaments wrapping around the bones and ligaments wrapping around each other (21). This is one of the few models which take these nonlinearities into account.

Lew and Lewis in 1977 and 1978 took an approach similar to Crowninshield's, although they applied an anthropometric scaling technique in order to determine the rotated coordinates of the attachments and scale them to the individual subject (23, 24). Using the locations of four bony landmarks on the tibia and fibula in cadaver and living subjects, they calculated a deformation gradient between the initial configuration in the cadaver and the final configuration in these living subjects' flexed limbs. The locations of the attachment points were thus mathematically transformed from the dissected cadaver limb to the inaccessible human subject's leg. They concluded from their testing that the straight line assumption was reasonable but

that the very small values of the changes in ligament length did present a problem in the accuracy of the model.

Wismans et al in 1980 again treated each of the ligaments as a straight, nonlinear spring (41). They also described the joint surfaces using a mathematical equation of the form

$$c = x\hat{i} + y_i(x, z)\hat{j} + z\hat{k}$$

They defined the ligament forces as a function of joint position, and used these relationships, along with equilibrium equations and contact equations derived from the mathematical description of the joint surface, to determine ligament forces, joint position, contact forces and locations, as a function of flexion angle and the applied "external forces and moments." These latter quantities consist of muscle as well as ground reaction forces and inertial quantities.

Andriacchi and others in 1983 developed a finite element model of the passive structures of the knee, treating the ligaments as 21 linear springs, the menisci (which most other investigators ignore) as two shear beam elements with shear bending and axial stiffness and the contact surfaces as ten hydrostatic elements which resist forces perpendicular to the surface (2). From this model these researchers were able to calculate total joint stiffnesses that agreed very well with experimental values.

Again, most of the work in this area has dealt with static or quasi-static models. One of the few examples of

dynamic models is the one presented by Moeinzadeh and other researchers in 1983 (27). This is a two-dimensional representation involving four ligaments. The dynamic equations of motion, contract conditions and the geometric compatibility of the problem are combined to obtain six non-linear differential equations with six unknowns. These equations are then solved for two arbitrary but simple "forcing functions" which represent the external forces and moments, including the total muscle force, applied to the system.

ANATOMICAL MODEL

In order to solve the problem of the force distribution in a joint, values for the attachment positions of the ligaments and muscles, as well as information concerning the joint surfaces and the points of joint contact, are necessary. This information is difficult to obtain due to the high degree of variability among individuals as well as the inaccessibility of the internal structures. In the past, investigators have relied on a variety of methods to assess these values, ranging from educated "guesses" based on anatomy texts, to radiographic and cadaver measurements. For this study, a model was developed based on values obtained from a variety of sources.

Several simplifying assumptions have been made in the formulation of the knee joint model. Some of the more basic of these are outlined as follows:

- 1) The tibia and fibula are assumed to be a single rigidly connected body. Any relative motion between them is ignored. Thus the terms shank, lower leg and tibia will be used interchangeably to refer to the body segment made up of these two bones.

- 2) With the exception of the quadriceps muscles whose directions are changed by the action of the patella, the

muscles and ligaments are assumed to act in a straight line between their assumed origins and insertions. The muscle origins and insertions are defined in such a way that errors due to this simplification are minimized.

3) The joint contact forces, or the forces at the bony articulations are assumed to act at a single point for each joint. Although in reality the area of contact can be a much larger region and for the knee two separate regions of contact, one on each condyle, are known to exist, any distribution of force can theoretically be reduced to a single equivalent force and moment acting in the same direction. If this moment is assumed to be negligible, which is reasonable considering the nature of the force distribution, a single force acting at a single point is a valid approximation.

4) While the problem is three-dimensional in nature, velocities and accelerations of motions out of the sagittal plane are assumed to be insignificant. This simplifies the dynamics of the problem without introducing significant errors since the terms involving these quantities make only a small contribution to the dynamic equations of motion. This assumption allows planar motion equations to be applied and eliminates the need to be concerned with the location of principal inertial axes or to develop the moment equations around the center of mass. Since the geometry of the problem is three-dimensional, with the forces displaying components in all three dimensions, static equilibrium

relationships can be used to relate the components in the remaining directions: i.e. if x points anteriorly, y laterally and z superiorly the equations of motion can be written in the form:

$$\sum F_x = ma_{cmx}$$

$$\sum F_y = 0.0$$

$$\sum F_z = ma_{cmz}$$

$$\sum M_x = 0.0$$

$$\sum M_y = I\alpha$$

$$\sum M_z = 0.0$$

Locations of muscle origins and insertion were calculated from data provided by Brand et al (5). This data was in the form of coordinates of the attachment points of each muscle in the local right-handed orthogonal reference frames indicated in Figure 1, scaled relative to various anthropometric measurements. This was nonhomogenous scaling in the sense that different measurements were used to scale each direction. Similar measurements taken from individual subjects could then be used to define a size transformation matrix to transform these coordinates to the corresponding coordinate reference frame in the individual.

Portions of muscles with broad origins or insertions were treated separately in order to account for varying effects of the various portions of the muscle. EMG data (Sodenberg and Dostal (36) for example) supports the idea that various portions function independently. For muscles which do not act in a straight line such as sartorius and

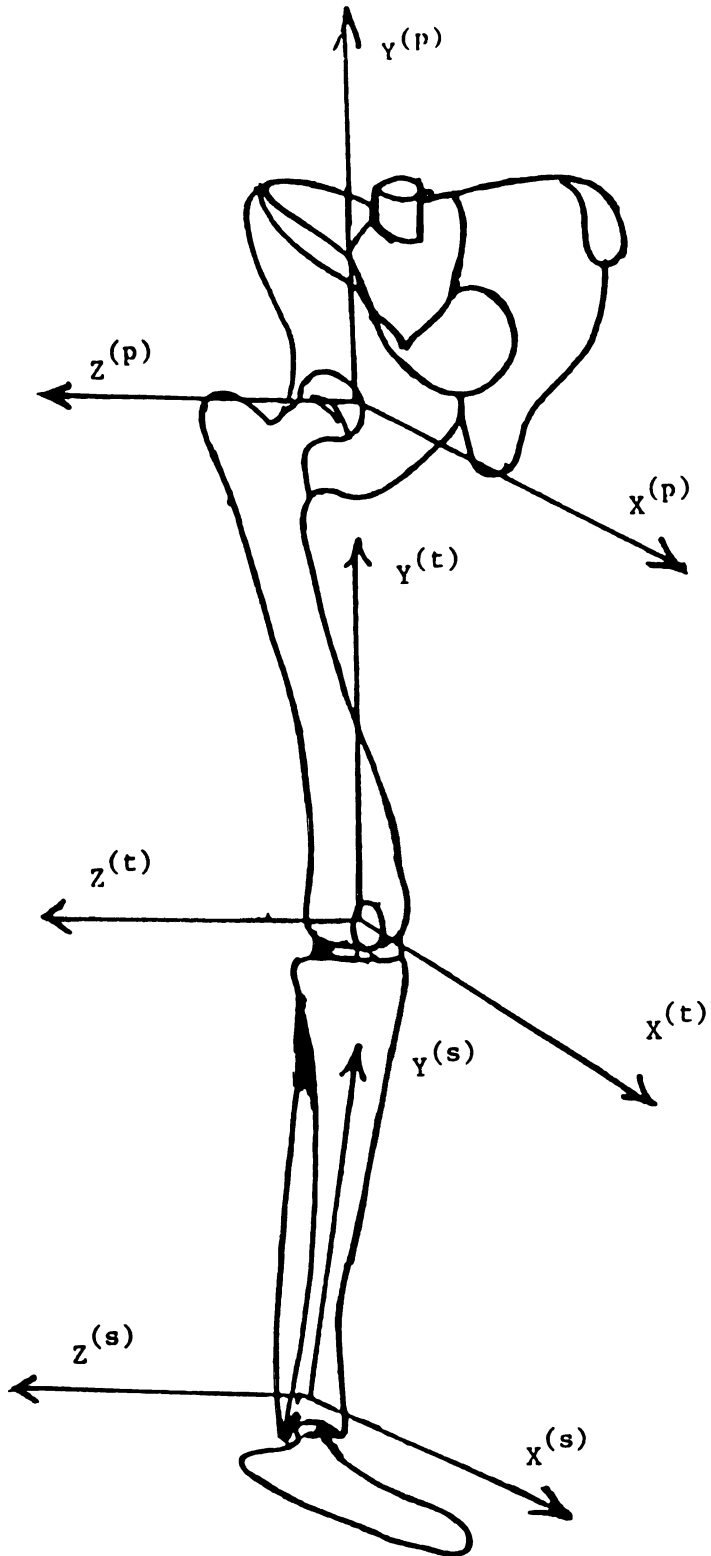


Figure 1. Local Coordinate Systems For the Description of Muscle Origins and Insertions

gracilis, effective origins or insertions were defined where the estimated centroid of the cross-section of the muscle or tendon crossed the joint (with the limb in anatomical position) and had the most realistic effect on the moment arm predictions.

Brand's scaled origin and insertion coordinates are shown in Table 1. Thirty-seven muscles or portions of muscles were included in this model. A comparison of the assumed muscle model with the actual musculature of the lower limb can be seen in Figure 2.

Brand's original scaling was based on anthropometric scale factors determined by radiographs for the pelvis and external bony landmarks for the femur and tibia. The measurements used are shown in Table 2. Adjustments were made to allow these values to be determined exclusively from external markers, hence the assumptions for the pelvic cephalic and frontal factors as percentages of the distance between the right and left ASIS's. Offsets due to soft tissue were also taken into account both in the determination of the bony coordinated systems and in determining scale factors. The details of these determinations are outlined in "A Three Dimensional Modeling to the Pelvic Limb" by Pendersen and Brand (31).

The vertical axis in Brand's tibial coordinate system is defined using the tibial tuberosity and the midpoint between the medial and lateral malleoli. In order to be consistent with the coordinate systems used in the remainder

Table 1. Scaled Local Coordinates of Muscle Attachments
(Brand's Data)

MUSCLE	<u>Origin</u>			<u>Insertion</u>		
	X	Y	Z	X	Y	Z
Biceps Femoris (long head)	-0.6206	-0.2370	-0.1888	-0.5884	1.0742	0.6863
Gracilis	0.4481	-0.2262	-0.8847	-0.9692	1.0923	-0.1333
Rectus Femoris	0.4852	0.1638	0.4944	-	-	-
Sartorius	0.7252	0.3231	1.0923	-0.8524	1.1075	-0.3240
Semimembranosus	-0.5668	-0.2246	-0.1614	-0.9018	1.0521	-0.0886
Semitendinosus	-0.6844	-0.2235	-0.1595	-0.9478	1.0917	-0.0682
Tensor Fasciae Latae	0.4819	0.4429	1.3515	-0.1587	1.1039	0.4869
Gastrocnemius (medial)	-0.2635	0.0186	-0.1920	-0.5649	-0.1371	0.0603
Gastrocnemius (lateral)	-0.2475	0.0116	0.2887	-0.5667	-0.1372	0.0594
Biceps Femoris(short)	-0.0086	0.4563	0.2832	-0.5897	1.0746	0.6888
Vastus Intermedius	0.2888	0.5253	0.3578	-	-	-
Vastus Lateralis	0.0148	0.5392	0.6861	-	-	-
Vastus Medialis	0.0483	0.4779	0.1730	-	-	-
Adductor Brevis 1	0.4611	-0.1927	-0.7865	-0.1126	0.7174	0.4125
Adductor Brevis 2	0.4822	-0.1917	-0.7882	-0.1451	0.6477	0.4068
Adductor Longus	0.7266	-0.1629	-0.7862	-0.0407	0.4858	0.2591
Adductor Magnus 1	-0.1810	-0.2785	-0.6454	-0.1542	0.6961	0.5411
Adductor Magnus 2	-0.1856	-0.2784	-0.6434	-0.0463	0.4351	0.3034
Adductor Magnus 3	-0.1850	-0.2776	-0.6447	-0.0768	0.0419	-0.5723
Gluteus Maximus 1	-0.4892	0.6544	-0.3505	-0.2023	1.0407	0.7167
Gluteus Maximus 2	-0.9664	0.4315	-0.5495	-0.2023	0.9262	0.7167
Gluteus Maximus 3	-1.0937	0.0682	-0.9122	-0.2023	0.7427	0.7167
Gluteus Medius 1	0.2462	0.4556	1.0205	-0.2329	0.9971	1.0869
Gluteus Medius 2	-0.3523	0.5470	0.2392	-0.2336	0.9977	1.0857
Gluteus Medius 3	-0.8096	0.3584	-0.3306	-0.2325	0.9976	1.0846
Gluteus Minimus 1	0.3508	0.3079	0.8956	-0.0853	0.9658	1.0814
Gluteus Minimus 2	-0.1228	0.3265	0.3571	-0.0842	0.9658	1.0801
Gluteus Minimus 3	-0.4348	0.2092	-0.0657	-0.0851	0.9659	1.0818
Iliacus	0.3022	0.2350	0.1228	-0.2200	0.8544	0.2070
Psoas	0.4675	0.0567	-0.1279	-0.2207	0.8548	0.2061
Inferior Gemelli	-0.6331	-0.0811	-0.1172	-0.1298	0.9975	0.8385
Obturator Externus	0.0821	-0.1419	-0.5320	-0.2963	0.9662	0.7647
Obturator Internus	-0.7265	-0.0444	-0.1603	-0.1307	0.9969	0.8348
Pectineus	0.4725	-0.0501	-0.3798	-0.1501	0.7985	0.4674
Piriformis	-0.8331	0.2902	-0.4803	-0.1829	1.0039	0.9366
Quadratus Femoris	-0.4774	-0.2364	-0.2910	-0.2205	0.8766	0.6147
Superior Gemelli	-0.6465	0.0043	-0.2423	-0.1304	0.9971	0.8321

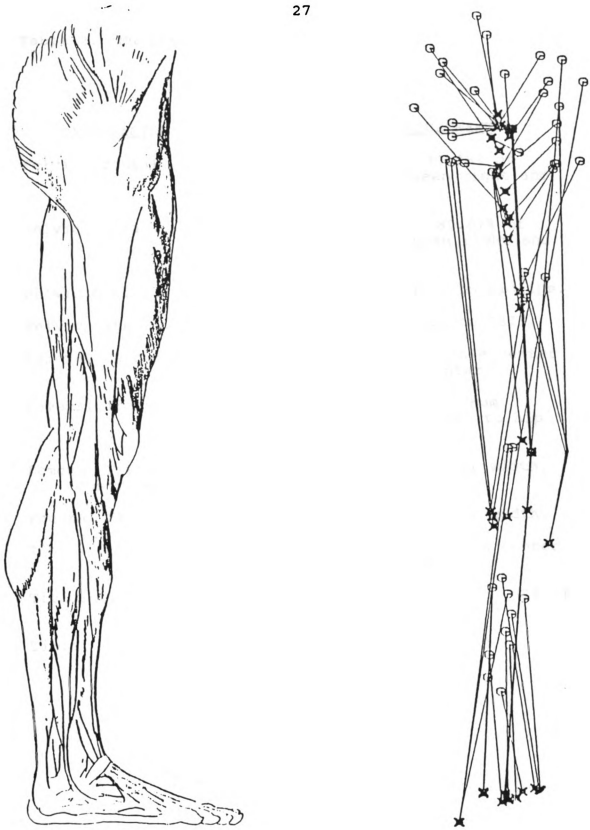


Figure 2. Comparison of Muscle Model to Actual Musculature of the Lower Limb

Table 2. Muscle Scale Factors

<u>SCALE FACTOR</u>	<u>MEASUREMENT</u>
Pelvic Frontal.....	Pelvic Depth, 43.98% of distance between right and left ASIS.
Pelvic Cephalic.....	Pelvic height, 80.67% of distance between right and left ASIS.
Pelvic Medial.....	Hip Joint center to midline.
Pelvic Lateral.....	Hip joint center to ASIS.
Femoral Cephalic.....	Femoral length, knee center to hip joint center.
Femoral Transverse.....	Lateral distance from greater trochanter to hip joint center.
Femoral Transverse,..... Gastronemius only	Femoral epicondylar width.
Femoral Frontal.....	Femoral epicondylar width.
Tibial Cephalic.....	Tibial length, ankle center to tibial tuberosity.
Tibial Transverse.....	Tibial plateau width, 92% of epicondylar width.
Tibial Frontal.....	Tibial plateau width

of this analysis, which take the axis connecting the center of the tibial plateau and the ankle center as the "vertical," Brand's original coordinate data for the tibial system was rotated by 7 degrees about the medial-lateral axis. This rotation is based on the assumed location of the tibial plateau center indicated in Figure 3.

The effect of the patella on knee moment arms was taken into account by modeling it as a single point at which the quadriceps muscles insert and the patellar ligament originates, effectively serving to change the direction of the action of these muscles. The local coordinates of the patella in the XY plane are defined for small flexion angles to be along the arc of a circle of radius 3.9 cm centered at the midpoint between the femoral epicondyles. The patellar radius is assumed to be 3.9 cm. At full extension, $X = 0$. For larger angles the quadriceps wrap around the femur maintaining a minimal distance of 2.2 cm from the knee joint center. For this situation the patella is assumed to be located at the point of intersection of a line parallel to and 2.2 cm from the Y axis and the tangent to the circle of radius 3.9 cm. As a result, in the femoral coordinates, for a flexion angle $\theta > \theta_c$:

$$\begin{aligned} X_p &= 2.2 \\ Y_p &= -3.9\sin\theta + (2.2-3.9\cos\theta)/\tan\theta \end{aligned}$$

and for $\theta < \theta_c$:

$$\begin{aligned} X_p &= 3.9\cos\theta \\ Y_p &= -3.9\sin\theta \end{aligned}$$

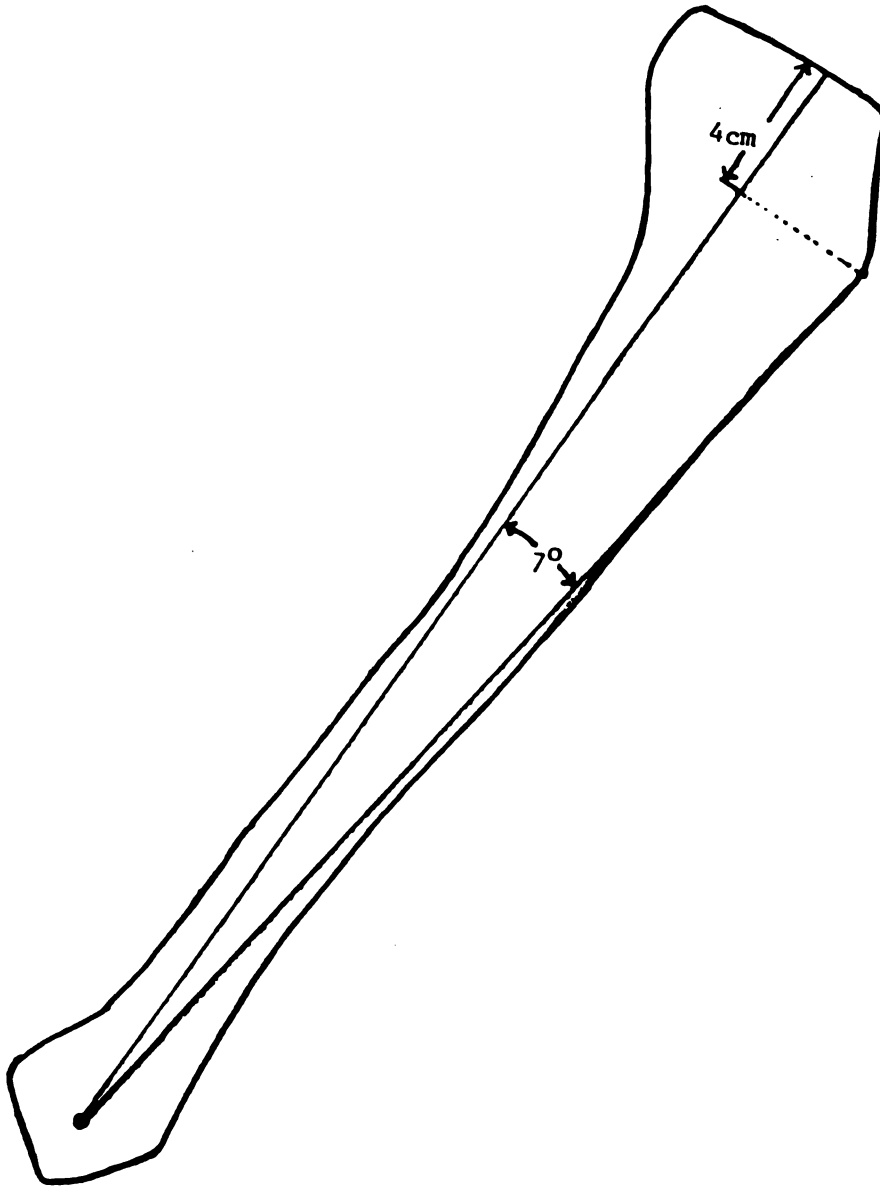


Figure 3. Assumed Relationship Between Tibial Tuberosity and Center of Tibial Plateau

where θ_c is the critical angle, defined to be $2.2 = 3.9\cos\theta_c$ or $\theta_c = 56^\circ$.

The Z coordinate of the patella, at all flexion angles, is assumed to be zero. The insertion of the patellar ligament on the tibia is located at the tibial tuberosity which in the tibial coordinate system is located along the Y axis. Its distance from the origin is the tibial cephalic scale factor.

It is reasonable to assume that the patella is in equilibrium. The patella thus exerts a force on the femur at the point of contact of the patello-femoral joint which is equal to the resultant of the quadriceps and the patellar ligament force.

$$(1) \quad F_{PAT} = F_3 + F_{11} + F_{12} + F_{13} - F_{PL}$$

where: F_{pat} = The force exerted on the femur by the patella

F_3 = The force exerted on the patella by rectus femoris

F_{11} = The force exerted on the patella by vasti intermedius

F_{12} = The force exerted on the patella by vasti lateralis

F_{13} = The force exerted on the patella by vasti medialis

$-F_{PL}$ = The force exerted on the patella by the patellar ligament

Since this force acts at the point of insertion of the quadriceps (and the origin of the patellar ligament), this known location can be used to calculate the effect that this force has on the dynamic equations of motion.

Experimentally it has been shown (Ellis et al in 1980 and Buff et al in 1988 (15, 8)) that a model of this joint which assumes that the patella acts as a frictionless pulley with $F_Q = F_P$ —where F_Q is the magnitude of the quadriceps force and F_P is the magnitude of the patellar ligament force, is not accurate for flexion angles greater than 30° . This difference is dictated by the geometry of the joint. In a two-dimensional model, F_P and F_Q being equal would require that the contact force be along the bisector of the angle formed by the lines of action of the quadriceps resultant and the patellar ligament. The contact force must also pass through the point of contact, which is not necessarily along the bisector. Both Buff and Ellis obtained similar experimental results for the ratio of the magnitudes of these two forces. In keeping with their findings it was assumed that:

$$(2) \quad S = F_Q/F_P = \begin{cases} 1.0 & \text{for } \theta < 30^\circ \\ -(0.4/60)\theta + 1.2 & \text{for } \theta > 30^\circ \end{cases}$$

In order to analyze this problem, it is also necessary to be able to calculate the stresses in each of the muscles. This required that values for the cross-sectional area of each be known. The physiological cross-section, which is defined as the volume of the muscle divided by its length, was used. Data for each of the individual muscles based on cadaver measurements of a 37-year-old subject was referenced from Brand and Pedersen (6). These values are contained in Table 3.

Table 3. Physiological Cross-Sectional Area of Individual Muscles

MUSCLE	PCSA (cm ²)
Biceps femoris(long head)	27.34
Gracilis	3.74
Rectus Femoris	42.96
Sartorius	2.90
Semimembranosus	46.33
Semitendinosus	13.05
Tensor Fasciae Latae	8.00
Gastrocnemius(medial)	50.60
Gastrocnemius(lateral)	14.30
Biceps Femoris(Short head)	8.14
Vastus Intermedius	82.00
Vastus Lateralis	64.41
Vastus Medialis	66.87
Adductor Brevis 1	11.52
Adductor Brevis 2	5.34
Adductor Longus	22.73
Adductor Magnus 1	25.52
Adductor Magnus 2	18.35
Adductor Magnus 3	16.95
Gluteus Maximus 1	20.20
Gluteus Maximus 2	19.59
Gluteus Maximus 3	20.00
Gluteus Medius 1	25.00
Gluteus Medius 2	16.21
Gluteus Medius 3	21.21
Gluteus Minimus 1	6.76
Gluteus Minimus 2	8.20
Gluteus Minimus 3	11.98
Iliacus	23.33
Psoas	25.70
Inferior Gemellus	4.33
Obturator Externus	2.71
Obturator Internus	9.07
Pectineus	9.03
Piriformis	20.54
Quadriceps Femoris	21.00
Superior Gemellus	2.13

The center of mass of the upper and lower leg are defined in the local coordinate system of the muscles as follows: The center of mass for each segment is assumed to lie along the y axis of the local coordinated system. For the upper leg, where this axis runs from the mid-point between the epicondyles to the hip joint center, the center of mass is assumed to be located 60.67% of the distance between these two points, measured from the distal location. The lower leg center of mass is taken to be 58.25% of the segment length. The segment length is taken to be the projection of the distance from the ankle to the tibial tuberosity (tibial cephalic scale factor) onto the vertical axis between the center of the tibial plateau and the ankle, plus 4 cm. The motivation for this definition can be seen from Figure 3.

Thirteen ligamentous structures are included in the model, these being various portions of the collaterals and cruciates as well as the joint capsule. Experimental considerations have shown that various portions of the individual ligaments function separately. Hence anterior and posterior portions of each cruciate are treated independently of each other, as are portions of the medial collateral and the capsule. The actual coordinates used, defined in coordinate systems associated with the femur and tibia, respectively, are indicated in Table 4. This data is based on the work of Crowninshield et al (11).

Table 4. Local Coordinates of Ligament Attachments.

LIGAMENT	Femoral			Tibial		
	X	Y	Z	X	Y	Z
Lateral Collateral	-3.99	3.5	-0.52cm	-2.50	4.50	11.27cm
Medial Collateral, posterior fibers	-3.79	-3.50	-0.02	-0.80	-2.00	9.77
Medial Collateral, anterior fibers	-2.29	-3.5	-0.02	0.70	-2.00	10.77
Medial collateral oblique	-3.29	-3.50	-0.02	-3.00	-3.50	13.77
Deep Medial Collateral	-2.99	-3.5	-0.32	0.00	-3.50	13.77
Posterior Cruciate, anterior fibers	-2.69	-0.50	-1.02	-2.50	-0.50	14.27
Posterior Cruciate, posterior fibers	-4.69	-0.5	-1.02	2.50	0.50	14.27
Anterior Cruciate, anterior fibers	-3.79	0.70	-0.52	0.50	-0.70	14.77
Anterior Cruciate, posterior fibers	-3.39	0.50	-0.52	0.20	0.00	14.77
Posterior Capsule, lateral fibers	-5.49	2.50	-0.02	-2.50	2.50	11.77
Posterior Capsule, medial fibers	-5.49	-2.50	-0.02	-2.50	-2.50	11.77
Oblique Posterior Capsule No. 1	-5.49	2.50	-0.02	-2.50	-2.50	11.77
Oblique Posterior Capsule No. 2	-5.49	-2.50	-0.02	-2.50	2.50	11.77

Each ligament was treated as a nonlinear spring with the constitutive relationship given by Crowninshield et al as well as by Grood and Hefzy:

$$(3) \quad F_{Li} = 750A \left(\frac{l - l_0}{l_0} \right)^2 N$$

where: A = the cross-sectional area of the ligament in mm² (these values are given in Table 5 for each of the ligaments)

l_0 = the unstretched or slack length of the ligament

l = the ligament length

Values for l_0 for each ligament were adapted from the work of Wismans et al (41). Wismans applied the relationship:

$$(4) \quad e_j = (l_j - l_0) / l_0$$

where e_j is the strain at full extension and l_j is the

length of the ligament at the same point. In terms of these equations:

$$(5) \quad l_o = l_j / (1 + e_j)$$

The values of e_j assumed for this study are contained in Table 5.

The two-dimensional representations of the joint surfaces presented by Moeinzadeh et al in 1983 were used in this analysis (27). In a tibial coordinate system defined as shown in Figure 4, with its origin at the center of mass of the segment, the tibial joint surface was represented by the nonlinear relationship:

$$(6) \quad Y_1 = f(x_1) = 0.14765 - 0.03156x_1 + 0.74282x_1^2$$

Similarly, the femoral surface was represented by

$$(7) \quad Y_2 = f(x_2) = 0.02778 - 0.17135x_2 - 4.7673x_2^2 - 187.1483x_2^3 - 5944.2399x_2^4$$

where the coordinate system, as defined in Figure 4, is assumed to have its origin at the midpoint of the line

Table 5. Ligament Parameters.

LIGAMENT	cross-section	e_j	l_o
Lateral Collateral	50.0mm ²	5.0%	59.67mm
Medial Collateral, posterior fibers	50.0	5.0%	77.52
Medial Collateral, anterior fibers	100.0	-3.0%	73.80
Medial collateral oblique	50.0	5.0%	45.96
Deep Medial Collateral	50.0	5.0%	35.24
Posterior Cruciate, anterior fibers	80.0	-1.0%	37.92
Posterior Cruciate, posterior fibers	80.0	-1.0%	28.37
Anterior Cruciate, anterior fibers	50.0	5.0%	29.97
Anterior Cruciate, posterior fibers	50.0	5.0%	24.94
Posterior Capsule, lateral fibers	40.0	5.0%	57.14
Posterior Capsule, medial fibers	40.0	5.0%	57.14
Oblique Posterior Capsule No. 1	10.0	5.0%	74.38
Oblique Posterior Capsule No. 2	10.0	5.0%	74.38

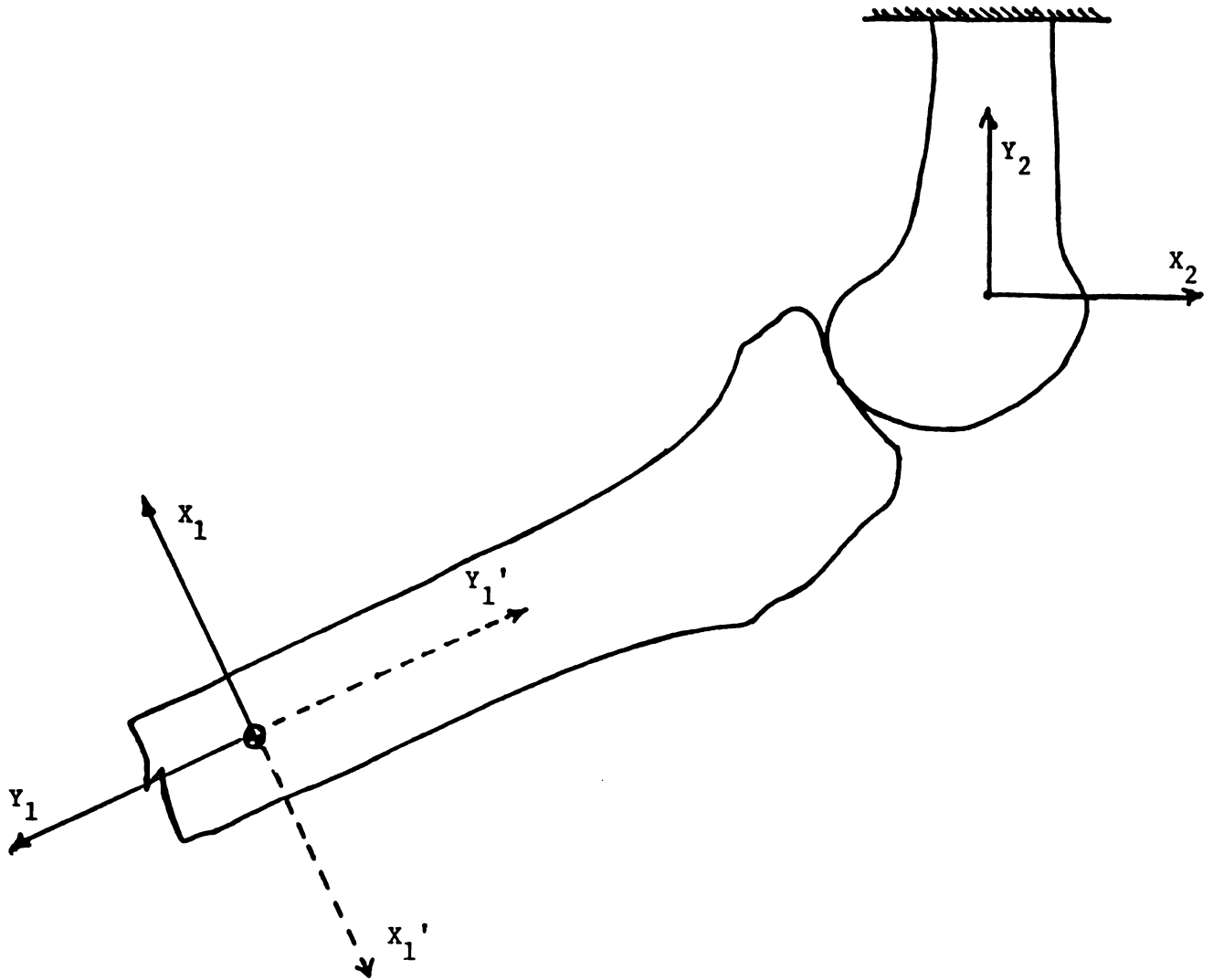


Figure 4. Two-Dimensional Joint Surfaces

connecting the medial and lateral epicondyles. The origins of both of these coordinate systems correspond with the origins of the coordinate systems used to define the location of the ligament attachments. A simple 180° rotation of the tibial system is all that is necessary to line up the coordinate axes as well.

In actuality, the tibia and femur have two separate regions of contact, one associated with each of the condyles. In order to include this two-dimensional representation of the joint surface in the three-dimensional model, the joint contact was assumed to be a single point and the x and y coordinates of the surface given above were assumed to hold only in the sagittal plane containing the contact point. The y coordinate of the contact point was assumed to be equal to zero in both the tibial and femoral coordinate system. Any medial-lateral translation of the tibia relative to the femur was thus ignored.

The single contact point assumed can then be represented in either the tibial or the femoral coordinate system such that

$$(8) \quad \{r_2\} = [Q]\{r_1\} + \{R_0\}$$

where: $\{r_1\}$ = A column vector representing the coordinates in the tibial system

$\{r_2\}$ = A column vector representing the coordinates in the femoral system

$\{R_0\}$ = A vector from the origin of the femoral system to the origin of the tibial system, in femoral coordinates.

[Q] = The rotation matrix describing the orientation of the tibia relative to the femur.

Additionally, in the two-dimensional representation the normal to the surfaces at any point can be expressed by

$$(9) \quad \hat{n}_1 = \frac{d^2 f_1 / dx_1^2}{|d^2 f_1 / dx_1^2|} \left[1 + \left(\frac{df_1}{dx_1} \right)^2 \right]^{-1/2} \left[\left(\cos \theta \frac{df_1}{dx_1} + \sin \theta \right) \hat{i} - \left(\cos \theta - \sin \theta \frac{df_1}{dx_1} \right) \hat{j} \right]$$

$$(10) \quad \hat{n}_2 = \frac{d^2 f_2 / dx_2^2}{|d^2 f_2 / dx_2^2|} \left[1 + \left(\frac{df_2}{dx_2} \right)^2 \right]^{-1/2} \left[\frac{df_2}{dx_2} \hat{i} - \hat{j} \right]$$

where \hat{i} and \hat{j} are the unit base vectors of the femoral system and θ is the angle of flexion or extension.

At the point of contact the normals must be colinear, requiring that the cross product of n_1 and n_2 be zero (i.e. $\hat{n}_1 \times \hat{n}_2 = 0$ at $x_1 = x_{c1}$ and $x_2 = x_{c2}$).

This contact condition then takes the form

$$(11) \quad \sin \theta \left(1 + \frac{df_2}{dx_2} \frac{df_1}{dx_1} \right) - \cos \theta \left(\frac{df_1}{dx_1} - \frac{df_2}{dx_2} \right) = 0$$

If the y component of the contact point in both coordinate systems is specified and the x component of the tibial contact point is also known, the contact condition along with the relationship between the two coordinate systems results in a system of four equations and four unknowns (R_{Ox}, R_{Oy}, R_{Oz} and x_{c2}).

The anterior-posterior position of the tibial contact point as a function of flexion angle was assumed as shown in Figure 5. This information was obtained from Iseki et al (22) as referenced by Mikosz et al (26).

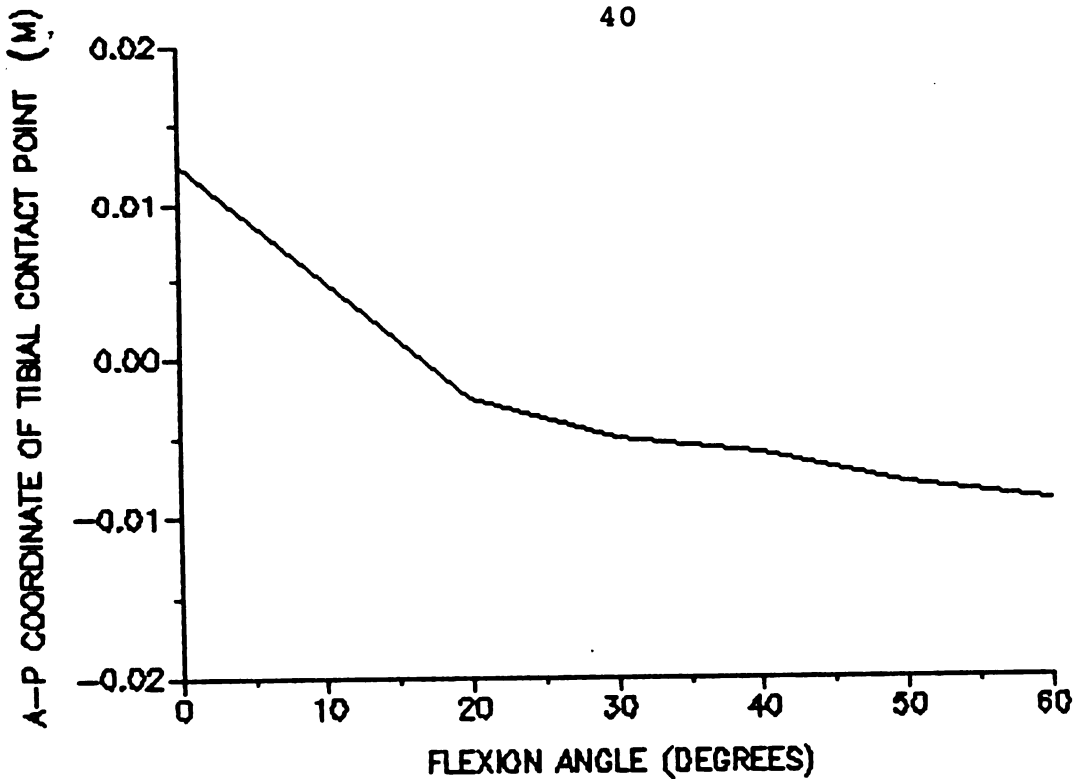


Figure 5. Anterior-Posterior Coordinate of Contact Point on Tibial Surface.

A simple hinge joint model of the knee was also developed for comparison purposes. For this case, a fixed rotation point was assumed. The aforementioned relationship between the representation of the joint contact point in the femoral and tibial coordinated systems remains applicable for the simpler model. The R_0 vector between the origins of the two systems, though, maintains a fixed magnitude for this case. Since the joint surface representations have no meaning for this model, the contact condition (equation 11) is no longer a valid relationship.

Once the local three-dimensional coordinates of the muscle and ligament attachments, the segment centers of mass

and the points of joint contact are known, it is necessary to transform them into a global or lab coordinate system. This lab system is defined such that the X axis points anteriorly, the Y axis laterally and the Z axis superiorly. The transformations can be carried out by:

$$(12) \quad \{R\} = [T]\{r\} + \{O\}$$

where: $\{r\}$ = The local coordinates of the point

$\{R\}$ = The global coordinates of the point

$\{O\}$ = The global coordinates of the origin of the local coordinate system

$[T]$ = the matrix representing the local coordinate axes system relative to the global system.
(Note: $[T_m]$ for the muscular coordinate system and $[T_l]$ for the ligament system differ slightly, due to the way these two reference frames were defined.)

This transformation gives the original unrotated or standing locations of these points.

To determine the position of the points with the leg in a flexed position, additional rotation matrices were defined to describe the orientation of the distal body segment relative to the more proximal, of the form:

$$[Q] = \begin{bmatrix} \cos\theta \cos\gamma + \sin\theta \sin\phi \sin\gamma & -\cos\phi \sin\gamma & \sin\theta \cos\gamma - \cos\theta \sin\phi \sin\gamma \\ \cos\theta \sin\gamma - \sin\theta \sin\phi \cos\gamma & \cos\phi \cos\gamma & \sin\theta \sin\gamma + \cos\theta \sin\phi \cos\gamma \\ -\sin\theta \cos\phi & -\sin\phi & \cos\theta \cos\phi \end{bmatrix}$$

where: θ = the angle of flexion at the knee and extension at the hip

ϕ = the angle of adduction

γ = the angle of external rotation

These angles are based on the assumption that in the standing position there was 0° of flexion, 0° of adduction and 0° of internal rotation.

In this analysis, the pelvic coordinate system was assumed to be held fixed in the global coordinate system. This is equivalent to assuming that the pelvic system maintains a fixed orientation in space and that the global coordinate system translates with the body as motion occurs. The coordinates of the origin of the femoral system were then rotated about the hip joint center such that:

$$(13) \quad \{O_2'\} = [Q_2]\{O_2-O_{hjc}\} + \{O_{hjc}\}$$

The location of the femoral coordinates in the flexed position are then described by:

$$(14) \quad \{R\} = [Q_2][T]\{r\} + \{O_2'\}$$

Since the rotations defined by $[Q_1]$ and $[Q_2]$ are relative to the location of the more superior body segment, points defined in the tibial system were first rotated by $[Q_2]$ and then by $[Q_1]$.

$$(15) \quad \{R\} = [Q_1][Q_2][T]\{r\} + \{O_1'\}$$

For the more general model, the center of rotation of the tibia relative to the femur is not a stationary point. The amount of sliding motion of the tibia relative to the femur is of interest, and a simple rotation of the coordinates of the origin of the tibial system about the origin of the femoral reference frame as was done previously for the femoral origin would not produce adequate results. An alternative approach is used. $\{R_0\}$ as previously defined

is a vector in the femoral coordinate system from the origin to the center of mass of the tibia. The location of the origin of the muscular tibial system is then:

$$(16) \quad \{O_1'\} = \{O_2'\} + [Q_2][T]\{R_O\} - [Q_1][Q_2][T]\{CM_1\}$$

where $\{CM_1\}$ is the location of the center of mass of the lower leg in the tibial coordinate system.

For the ligamentous coordinate system, the analysis differs only in that the origin is located at the center of mass, resulting in the new global coordinates of the origin being defined by:

$$(17) \quad \{O_1'\} = \{O_2'\} + [Q_2][T_1]\{R_O\}$$

With the above analysis, it is thus possible to calculate the global coordinates of all attachment points, both muscular and ligamentous, as well as the positions of other important points such as the segment centers of mass and joint contact points, in any limb configuration specified. By knowing the orientations of each of the body segments, the line of action and points of application of the various internal forces can be found.

ANALYTICAL METHODS

By treating each segment of the limb as a free body, subject to the laws of Newtonian mechanics, the total external joint moments and forces at the ankle, knee and hip can be determined from the equations of motion. Assuming that velocities and accelerations outside the sagittal plane are insignificant, the relationships for planar motion can be applied. Articulating segments, as represented in Figure 6, exert equal and opposite forces and moments on each other, resulting in the following relationships.

For the foot:

$$(1) \quad F_A + F_{GR} - W^{(f)} = m^{(f)} a_{cm}^{(f)}$$

$$(2) \quad M_A + M_{GR} + R^{(f)} \times F_{GR} - p_{cm}^{(f)} \times W^{(f)} = \\ I^{(f)} \alpha^{(f)} + p_{cm}^{(f)} \times m^{(f)} a_{cm}^{(f)}$$

For the shank:

$$(3) \quad F_K - F_A - W^{(s)} = m^{(s)} a_{cm}^{(s)}$$

$$(4) \quad M_K - M_A - R^{(s)} \times F_A - p_{cm}^{(s)} \times W^{(s)} = \\ I^{(s)} \alpha^{(s)} + p_{cm}^{(s)} \times m^{(s)} a_{cm}^{(s)}$$

For the thigh:

$$(5) \quad F_H - F_K - W^{(t)} = m^{(t)} a_{cm}^{(t)}$$

$$(6) \quad M_H - M_K - R^{(t)} \times F_K - p_{cm}^{(t)} \times W^{(t)} = \\ I^{(t)} \alpha^{(t)} + p_{cm}^{(t)} \times m^{(t)} a_{cm}^{(t)}$$

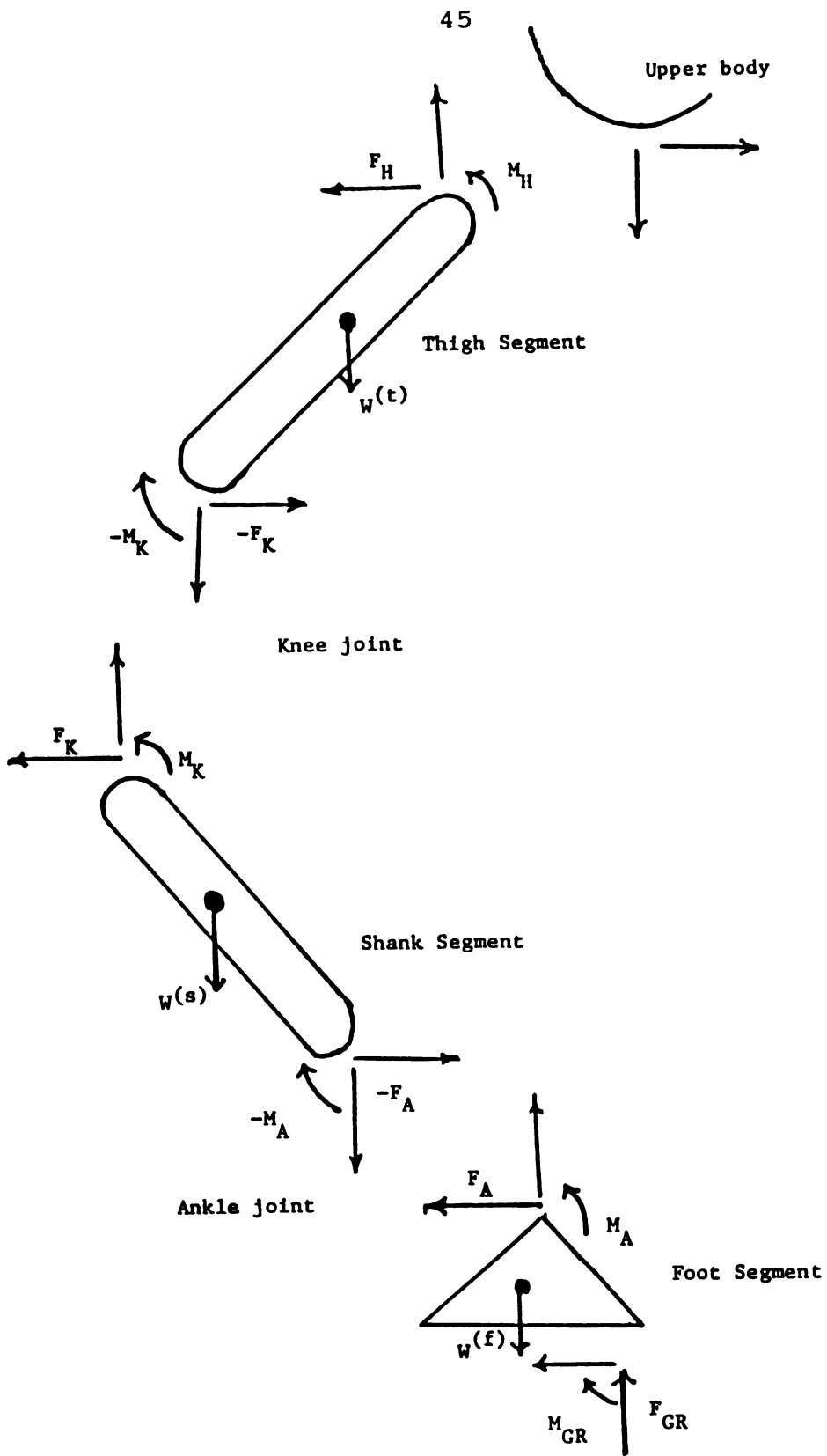


Figure 6. External Joint Forces and Moments

where:

F_{GR} = The ground reaction force as exerted on the foot

M_{GR} = The moment associated with the ground reaction

F_A = The total joint force at the ankle

M_A = The total joint moment at the ankle

F_K = The total joint force at the knee

M_K = The total joint moment at the knee

F_H = The total joint force at the hip

M_H = The total joint moment at the ankle

R = A vector from the proximal to the distal joint center

p_{cm} = A vector from the proximal joint center to the center of mass of the segment

W = The weight of the segment, assumed positive downward

Note: the superscripts (f), (s) and (t) indicate values associated with the foot, shank and thigh respectively.

The ground reaction forces can be measured using a force platform and the kinematic variables by means of high-speed stereo-cine photography. From these relationships it is then possible to determine the total force and moment acting at each joint.

Internally these total joint forces and moments are carried by the individual muscles and ligaments crossing the joint, as well as by the contact force exerted by the articulating bony surfaces on each other. Unlike the ligament and contact forces, even when the muscles are assumed to act in a straight line between their origin and insertion, the forces produced by the muscles do not

necessarily exert equal and opposite forces on the articulating body segments. This is due to the fact that many of these structures cross more than one joint and act on body segments which have no direct articulation with each other. The muscles acting in the lower limb, excluding the quadriceps, can be separated as follows into five groups based on the bony structures between which they act:

those acting between:

- 1) The foot and the tibia
- 2) The foot and the femur
- 3) The tibia and the femur
- 4) The tibia and the pelvic region
- 5) The femur and the pelvic region

The total forces produced by each of these classifications can be represented by F_1 , F_2 , F_3 , F_4 and F_5 respectively.

The quadriceps muscles, rectus femoris, vastus medialis, vastus intermedius and vastus lateralis, which act on the tibia via the patellar tendon, must be treated separately. The interaction of these muscles on the patella effectively results in a change in the direction of the muscle force. In addition, a force, equal to the resultant of the forces in the quadriceps and the patellar tendon, is exerted on the femur by the patella. One of the quadriceps, the rectus femoris, is a two joint muscle, acting on the patella and the pelvis, while the remainder spans a single joint. If these two classifications are represented as F_{Q2}

and F_{Q1} , respectively, and if the force carried by the patellar ligament is represented by F_{p1} , then the force exerted on the femur by the patella can be written as:

$$(7) \quad F_{PAT} = F_{Q1} + F_{Q2} - F_{PL}$$

Since the quadriceps were all assumed to insert at the same point on the patella, the origin of patellar ligament, F_{PAT} can also be assumed to act through that point.

Referring to Figure 7, the following equations of motion can be written. As before, all motions are assumed to be in the sagittal plane and both the muscles and ligaments are assumed to act in straight line between their origin and insertion points.

For the foot:

$$(8) \quad F_{La} + F_{Ca} + F_{GR} + F_1 + F_2 - W^{(f)} = m^{(f)} a_{cm}^{(f)}$$

$$(9) \quad M_{La} + M_{GR} + R^{(f)} \times F_{GR} + r_1^{(f)} \times F_1 + r_2^{(f)} \times F_2 = \\ I^{(f)} \alpha^{(f)} + p_{cm}^{(f)} \times (m^{(f)} a_{cm}^{(f)} + W^{(f)})$$

For the shank:

$$(10) \quad F_{Lk} + F_{ck} - F_{La} - F_{Ca} - F_1 + F_3 + F_4 + F_{PL} - W^{(s)} \\ = m^{(s)} a_{cm}^{(s)}$$

$$(11) \quad M_{Lk} - M_{La} - R^{(s)} \times F_{La} - R^{(s)} \times F_{Ca} - r_1^{(s)} \times F_1 \\ + r_3^{(s)} \times F_3 + r_4^{(s)} \times F_4 + r_{PL}^{(s)} \times F_{PL} = \\ I^{(s)} \alpha^{(s)} + p_{cm}^{(s)} \times (m^{(s)} a_{cm}^{(s)} + W^{(s)})$$

For the thigh:

$$(12) \quad F_{Lh} + F_{ch} - F_{Lk} - F_{ck} - F_2 - F_3 + F_5 - F_{Q1} + F_{PAT} \\ - W^{(t)} = m^{(t)} a_{cm}^{(t)}$$

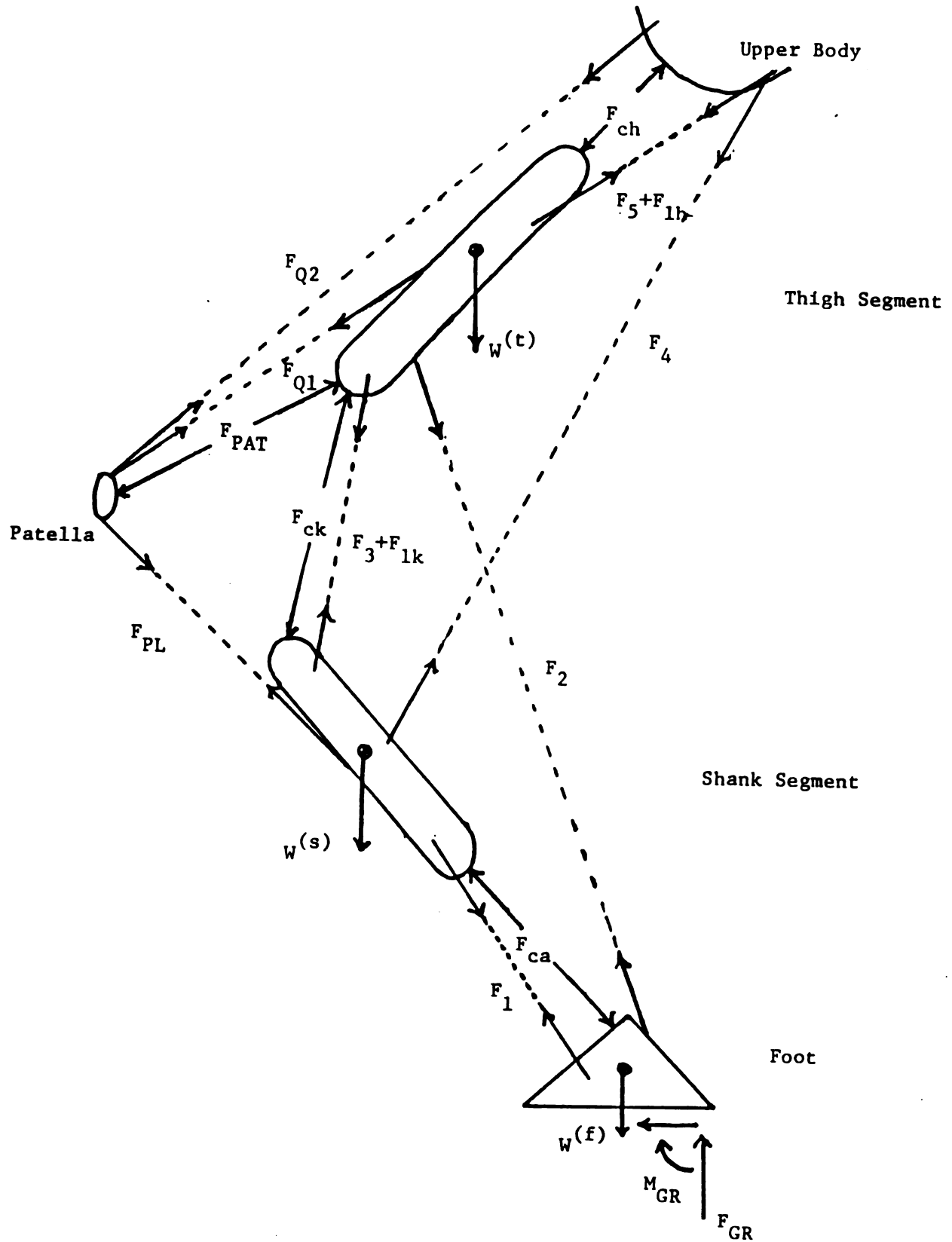


Figure 7. Free Body Diagram of Forces Acting on the Lower Limb

$$\begin{aligned}
 (13) \quad M_{Lh} - M_{Lk} - R^{(t)} \times F_{Lk} - R^{(t)} \times F_{ck} - r_2^{(t)} \times F_2 \\
 - r_3^{(t)} \times F_3 + r_5^{(t)} \times F_5 - r_{Q1}^{(t)} \times F_{Q1} + r_{PAT}^{(t)} \times F_{PAT} \\
 = I^{(t)} \alpha^{(t)} + p_{cm}^{(t)} \times (m^{(t)} a_{cm}^{(t)} + W^{(t)})
 \end{aligned}$$

where F_{La} = The resultant of the force carried by ligaments at the ankle

F_{ca} = The contact force at the ankle

F_{GR} = The ground reaction force exerted on the foot

M_{La} = The moment around the point of contact carried by the ligaments of the ankle

M_{GR} = The moment due to the ground reaction

F_{Lk} = The resultant of the force carried by the ligaments at the knee

F_{ck} = The contact force at the knee

M_{Lk} = The moment around the point of contact carried by the ligaments of the knee

F_{Lh} = The resultant of the force carried by the ligament at hip

F_{ch} = The contact force at the hip

M_{Lh} = The moment around the hip joint center carried by the ligaments of the hip

R = A vector from the proximal joint contact to the distal

r_i = A vector from the proximal joint contact to a point along the line of action of an applied force i

As before, (f), (s) and (t) indicate quantities associated with the foot, shank and thigh. All forces which act between two points are represented as positive at their most distal point of application and negative at the more proximal.

If it is recognized, by comparing equations 1 and 2 with 8 and 9, that the total joint force acting at the ankle

is equivalent to the sum of F_{La} , F_1 , F_2 and F_{Ca} and, by a similar comparison, that the total joint moment can be expressed in terms of M_{La} , F_1 and F_2 , the following relationships can be written:

$$(14) \quad F_A = F_{La} + F_{Ca} + F_1 + F_2$$

$$(15) \quad M_A = M_{La} + r_1^{(f)} \times F_1 + r_2^{(f)} \times F_2$$

Making the substitutions:

$$(16) \quad F_A - F_2 = F_{La} + F_{Ca} + F_1$$

$$(17) \quad M_A - r_2^{(f)} \times F_2 = M_{La} + r_1^{(f)} \times F_1$$

and recognizing that for any force, F , with a line of action which can be located relative to two points A and B by r_A and r_B , the moment around A can be represented as the sum of the moment around B and the moment around A caused by an equivalent force acting at B. In other words, as represented in Figure 8:

$$(18) \quad r_A \times F = R \times F + r_B \times F$$

or

$$(19) \quad r_A \times F = R \times F + M_B$$

From this elementary relationship it can be shown that, for the problem in question:

$$(20) \quad r_i^{(s)} \times F_i = R^{(s)} \times F_i + r_i^{(f)} \times F_i$$

$$(21) \quad r_i^{(t)} \times F_i = R^{(t)} \times F_i + r_i^{(s)} \times F_i$$

Equations 10 and 11, thus, reduce to:

$$(22) \quad F_{Lk} + F_2 + F_3 + F_4 + F_{PL} = m^{(s)} a_{cm}^{(s)} + W^{(s)} - F_{ck} + F_A$$

$$(23) \quad M_{Lk} + r_2^{(s)} \times F_2 + r_3^{(s)} \times F_3 + r_4^{(s)} \times F_4 + r_{PL}^{(s)} \times F_{PL} = I^{(s)} \alpha^{(s)} + p_{cm}^{(s)} \times (m^{(s)} a_{cm}^{(s)} + W^{(s)}) + M_A + R^{(s)} \times F_A$$

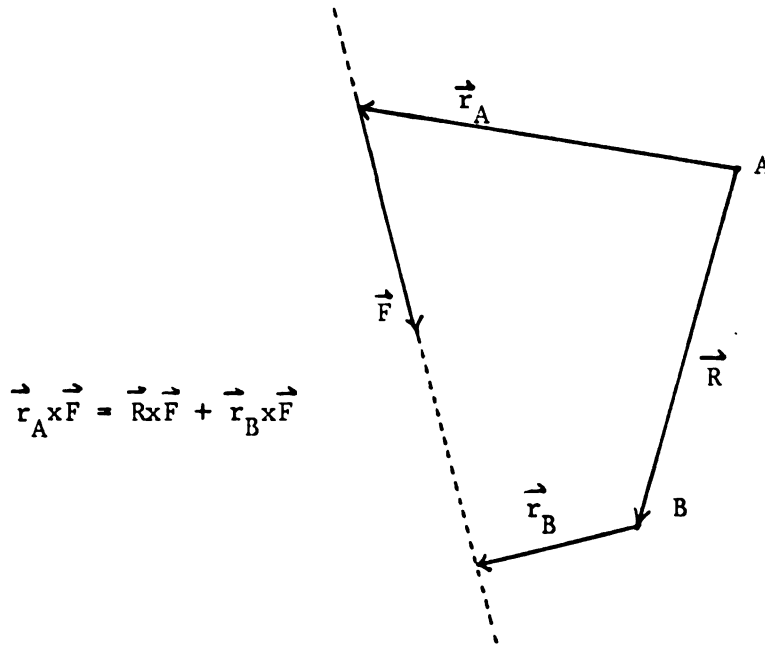


Figure 8. Moment Relationship.

Similarly, for the equilibrium relationships associated with the thigh segment, if the equations:

$$(24) \quad F_{Lk} + F_{ck} + F_2 + F_3 = F_K - F_4 - F_{PL}$$

$$(25) \quad M_{Lk} + r_2^{(s)} \times F_2 + r_3^{(s)} \times F_3 = M_K - r_4^{(s)} \times F_4 - F_{PL}^{(s)} \times F_{PL}$$

are substituted, the following results:

$$(26) \quad F_{Lh} + F_{ch} - F_K + F_4 + F_{PL} + F_5 - F_{Q1} + F_{PAT} - W(t) = m(t) a_{cm}(t)$$

$$(27) \quad M_{Lh} - M_K - R(t) \times F_K + r_4(t) \times F_4 + r_5(t) \times F_5 + r_{PL}(t) \times F_{PL} - r_{Q1}(t) \times F_{Q1} + r_{PAT}(t) \times F_{PAT} = I(t) \alpha(t) + p_{cm}(t) \times (m(t) a_{cm}(t) + W(t))$$

The moment contribution of the ligaments at the hip was assumed to be insignificant, thus $M_{Lh} = 0$. Also, since,

$F_{PAT} = F_{Q1} + F_{Q2} - F_{PL}$ and $r_{PAT}^{(t)}$, associated with the patellar contact force, is along the line of action of each of the forces F_{Q1} , F_{Q2} and F_{PL} , and F_K and M_K can be represented in terms of F_A , M_A and inertial values as indicated in equations 3 and 4, the above equations reduce to :

$$(28) \quad F_4 + F_5 + F_{Q2} = m^{(t)} a_{cm}^{(t)} + W^{(t)} + m^{(s)} a_{cm}^{(s)} + W^{(s)} - F_{ch} + F_A$$

$$(29) \quad r_4^{(t)} \times F_4 + r_5^{(t)} \times F_5 - r_{Q2}^{(t)} \times F_{Q2} = I^{(t)} \alpha^{(t)} + p_{cm}^{(t)} \times (m^{(t)} a_{cm}^{(t)} + W^{(t)}) + I^{(s)} \alpha^{(s)} + (p_{cm}^{(s)} + R^{(t)}) \times (m^{(s)} a_{cm}^{(s)} + W^{(s)}) + M_A + (R^{(t)} + R^{(s)}) \times F_A$$

The purpose of this analysis is to determine the forces in the individual structures in the lower limb which cross the knee joint. The majority of the muscles which cross the knee also cross the hip. The motions which result from the excitation of these two joint muscles are somewhat ambiguous and are affected by the relative positions and actions of both joints. Treating the knee in a completely isolated sense is therefore not practical. This is supported by the equations which have been developed.

As has been shown, if the assumption of straight line action is made, the muscles which cross only the ankle can be ignored. Their effect can be completely accounted for in the total muscle force and moment at the ankle (F_A and M_A). This leaves 12 remaining equilibrium equations, relating the components of the muscle forces and ligament forces.

Reserving the force equations for the determination of the unknown components of the contact forces, only the six moment equations remain, relating the moments carried by the muscles and ligaments crossing the joint with the external moments at each joint.

The line of action and the moment arm about the assumed joint center can be determined from the global coordinates of the muscle origin and insertions points derived as outlined in the previous section. From these the unit moment of each muscle about the joint center can be calculated. Equations 23 and 29 can then be written in the form:

$$(30) \quad \begin{bmatrix} K \\ 6 \times 38 \end{bmatrix} \begin{bmatrix} f_1 \\ f_2 \\ f_3 \\ \cdot \\ \cdot \\ \cdot \\ f_{38} \\ 38 \times 1 \end{bmatrix} = \begin{bmatrix} B \\ 6 \times 1 \end{bmatrix}$$

where: $K_{1i} = r_{yz} - r_{zy}$; or 0 if muscle i does not cross the joint

$$K_{2i} = r_{zx} - r_{xz}; \text{ or } 0$$

$$K_{3i} = r_{xy} - r_{yx}; \text{ or } 0$$

$$K_{4i} = r_{yz} - r_{zy}; \text{ or } 0$$

$$K_{5i} = r_{zx} - r_{xz}; \text{ or } 0$$

$$K_{6i} = r_{xy} - r_{yx}; \text{ or } 0$$

(Note: x , y and z are the direction cosines of the line of action of each individual muscle)

$$\begin{aligned}
B_1 &= p_{cmy}^{(s)} (m^{(s)} a_{cmz}^{(s)} + w^{(s)}) + R_Y^{(s)} F_{AZ} \\
&\quad - R_Z^{(s)} F_{AY} + M_{AX} - M_{LX} \\
B_2 &= I^{(s)} \alpha^{(s)} + p_{cmz}^{(s)} m^{(s)} a_{cmx}^{(s)} - \\
&\quad p_{cmx}^{(s)} (m^{(s)} a_{cmz}^{(s)} + w^{(s)}) + \\
&\quad R_Z^{(s)} F_{AX} - R_X^{(s)} F_{AZ} + M_{AY} - M_{LY} \\
B_3 &= -p_{cmy}^{(s)} m^{(s)} a_{cmx}^{(s)} + R_X^{(s)} F_{AY} - R_Y^{(s)} F_{AX} \\
&\quad + M_{AZ} - M_{Lz} \\
B_4 &= p_{cmy}^{(t)} (m^{(t)} a_{cmz}^{(t)} + w^{(t)}) \\
&\quad + p_{cmy}^{(s)} (m^{(s)} a_{cmz}^{(s)} + w^{(s)}) \\
&\quad + (R_Y^{(t)} + R_Y^{(s)}) F_{AZ} - (R_Z^{(t)} + R_Z^{(s)}) F_{AY} \\
&\quad + M_{AX} - M_{LX} \\
B_5 &= I^{(t)} \alpha^{(t)} + I^{(s)} \alpha^{(s)} + p_{cmz}^{(t)} m^{(t)} a_{cmx}^{(t)} \\
&\quad - p_{cmx}^{(t)} (m^{(t)} a_{cmz}^{(t)} + w^{(t)}) \\
&\quad + p_{cmz}^{(s)} m^{(s)} a_{cmx}^{(s)} - p_{cmx}^{(s)} (m^{(s)} a_{cmz}^{(s)} + w^{(s)}) \\
&\quad + (R_Z^{(t)} + R_Z^{(s)}) F_{AX} - (R_X^{(t)} + R_X^{(s)}) F_{AZ} \\
&\quad + M_{AY} - M_{LY} \\
B_6 &= -p_{cmy}^{(t)} m^{(t)} a_{cmx}^{(t)} - p_{cmy}^{(s)} m^{(s)} a_{cmx}^{(s)} \\
&\quad + (R_X^{(t)} + R_X^{(s)}) F_{AY} - (R_Y^{(t)} + R_Y^{(s)}) F_{AX} \\
&\quad + M_{AZ} - M_{Lz}
\end{aligned}$$

and the f_i 's are the individual magnitude of the forces in the 37 muscles as well as the force carried by the patellar ligament (f_{38}).

Since the muscle model includes 38 different structures in addition to the 13 ligamentous components this results in a highly underdetermined system.

The individual ligament loading can be calculated in terms of the joint position, such that:

$$(31) \quad F_{Li} = \begin{cases} 750A \left(\frac{l - l_0}{l_0} \right)^2 & \text{if } l > l_0 \\ 0 & \text{if } l \leq l_0 \end{cases}$$

where: A = The ligament cross sectional area, in mm²

l_0 = The original slack length of the ligament

l = The active length of the ligament

$$= \sqrt{[(R) - [T](r) - (R_0)] [(R) - [T](r) - (R_0)]}$$

Note: (R) and (r) are the femoral and tibial ligament attachments, respectively, and [T] and (R₀) are as defined previously.

The total ligament moment components in equation 30 are then given by:

$$(32) \quad M_{Lx} = \sum (r_y z - r_z y) F_{Li}$$

$$(33) \quad M_{Ly} = \sum (r_z x - r_x z) F_{Li}$$

$$(34) \quad M_{Lz} = \sum (r_x y - r_y x) F_{Li}$$

From the infinite number of combinations of muscle loadings, the solution which maximizes the endurance time was chosen. This corresponds to Crowninshield and Brand's optimization criterion of minimizing the sum of the cubes of the muscle stresses. The objective function was normalized by taking its cube root. This resulted in the cost function displaying the units of muscle stress and also prevented possible errors associated with disproportionately large objective values.

Additional constraints were also formulated in order to relate the quadriceps muscle force with the load carried by the patellar ligament as well as to constrain the knee

contact force to act normal to the joint surface. These relations are:

$$(35) \quad S \cdot |\vec{F}_{PL}| - |\vec{f}_3 + \vec{f}_{11} + \vec{f}_{12} + \vec{f}_{13}| = 0$$

$$(36) \quad \vec{F}_{\text{cshear}} = \vec{F}_{\text{ck}} - (\hat{n} \cdot \vec{F}_{\text{ck}}) \hat{n} = 0$$

where S is the assumed ratio of the patellar ligament load to the quadriceps force, \hat{n} is found as outlined in the previous section and F_{ck} is given by rearrangement of equation 22. The latter constraint was relaxed in this problem formulation so that the shear component of the contact force as calculated was simply required to be less than 10% of the total joint contact force. The value of 10% was chosen arbitrarily to allow for slight variations in the joint surface geometry. All muscle forces were also required to be nonnegative. This constraint is due to the physiological fact that muscles are only capable of producing tensile loading. An upper bound corresponding to a muscle stress of 100 N/cm² was also placed on each muscle force.

The statement of this problem is then:

Find \underline{F} that:

$$(37) \quad \text{minimizes } \Phi(\underline{F}) = \left(\sum (f_i/A_i)^3 \right)^{1/3}$$

subject to:

$$0 \leq f_i/A_i \leq 100 \text{ N/cm}^2$$

the equilibrium equations (30)

quadriceps relation (35)

$$|\vec{F}_{\text{cshear}}|/|\vec{F}_{\text{ck}}| \leq 0.1$$

A generalized reduced gradient algorithm, as outlined in the appendix, was then used to find the solution to this problem.

RESULTS AND DISCUSSION

The problem formulated in the previous sections was solved at discrete time intervals in the stance phase of gait for a female subject, 16 years of age and weighing 100 pounds. The scale factors, based on anthropometric measurements, shown in Table 6 were used to transform Brand's muscle origin and insertion data into the subject's own local coordinate systems, and develop a realistic representation of the individual's musculature.

Kinematic and kinetic inputs to the model such as linear and angular accelerations of the body segments, ground reaction forces and joint angles were calculated from three-dimensional film and force data collected as the subject ran barefooted across a force platform. The measured ground reaction forces and moments were transferred to the ankle center, taking into account the inertial effects of the motion of the foot in the sagittal plane, in order to obtain values for F_A and M_A . Figure 9 shows these moment components acting at the ankle. Knee angles, representing flexion-extension, abduction-adduction and internal-external rotation were calculated using a joint coordinated analysis(18) and are shown in Figure 10. Due to the lack of data with which to calculate three-dimensional

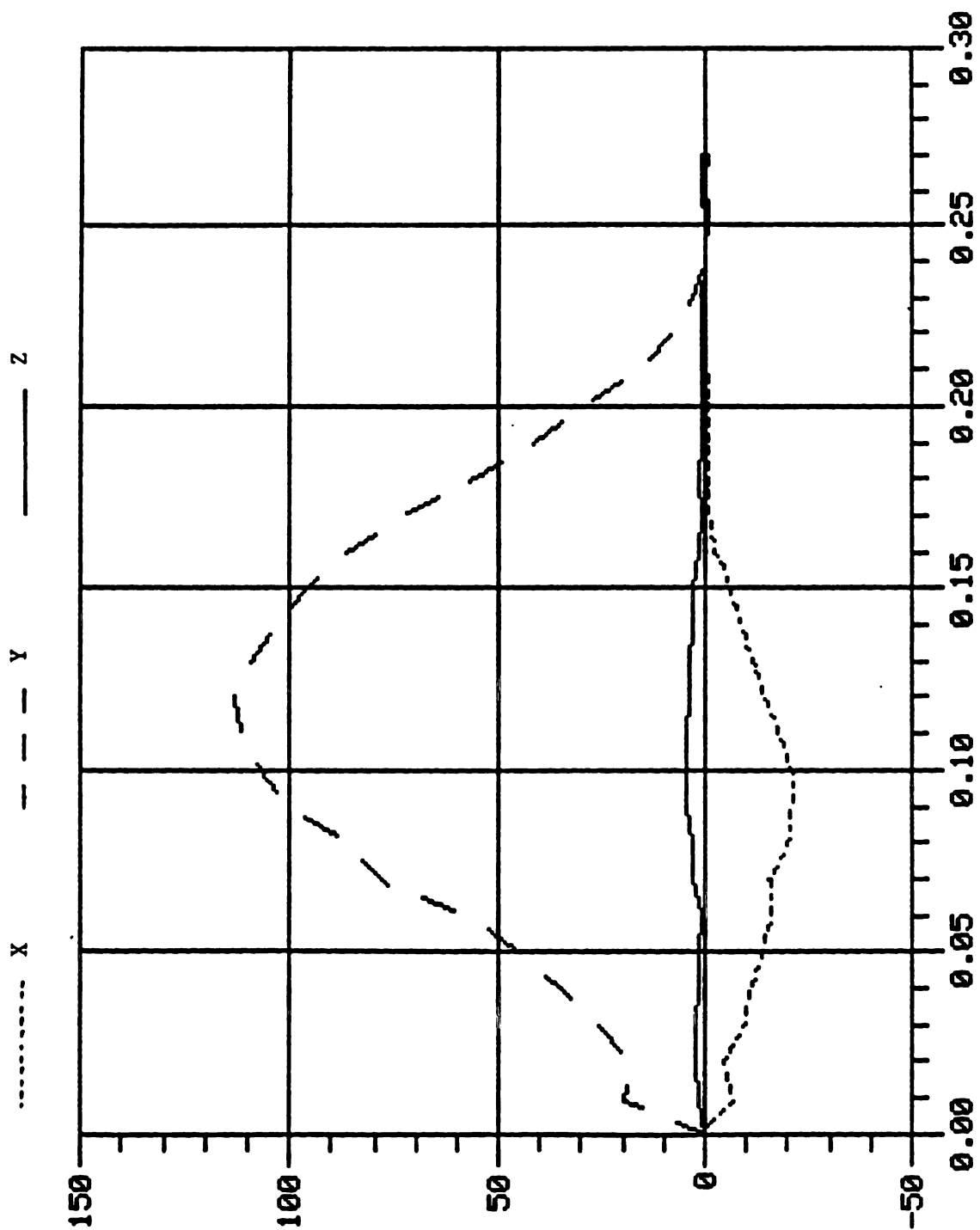


Figure 9. Ankle Moments

Table 6. Actual Subject Scale Factors

<u>SCALE FACTOR</u>	<u>MEASUREMENT</u>
Pelvic Frontal	11.52 cm
Pelvic Cephalic	21.11
Pelvic Medial	8.15
Pelvic Lateral	4.95
Femoral Cephalic	38.24
Femoral Transverse	4.63
Femoral Transverse, Gastrocnemius only	8.91
Femoral Frontal	8.91
Tibial Cephalic	31.61
Tibial Transverse	8.20
Tibial Frontal	8.20

hip angles, the orientation of this joint was expressed in terms of the flexion-extension angles seen in Figure 11 only.

In this model the ligament contribution to the moment at the knee depends solely on the relative orientation of the tibia and femur. To demonstrate the model under passive conditions, for flexion angles between 0° and 50° , the inherent internal rotation of the tibia associated with the screw home mechanism of the knee was assumed to be a function of the fifth root of the angle of flexion. This relation was based on Crowninshield's observations (11). The extension ratios at each flexion angle are displayed in Figure 12. These values are the ratio of the calculated ligament length in the rotated position and the original slack length, l_0 , calculated as outlined in a previous section. It should be noted that in the cases where this

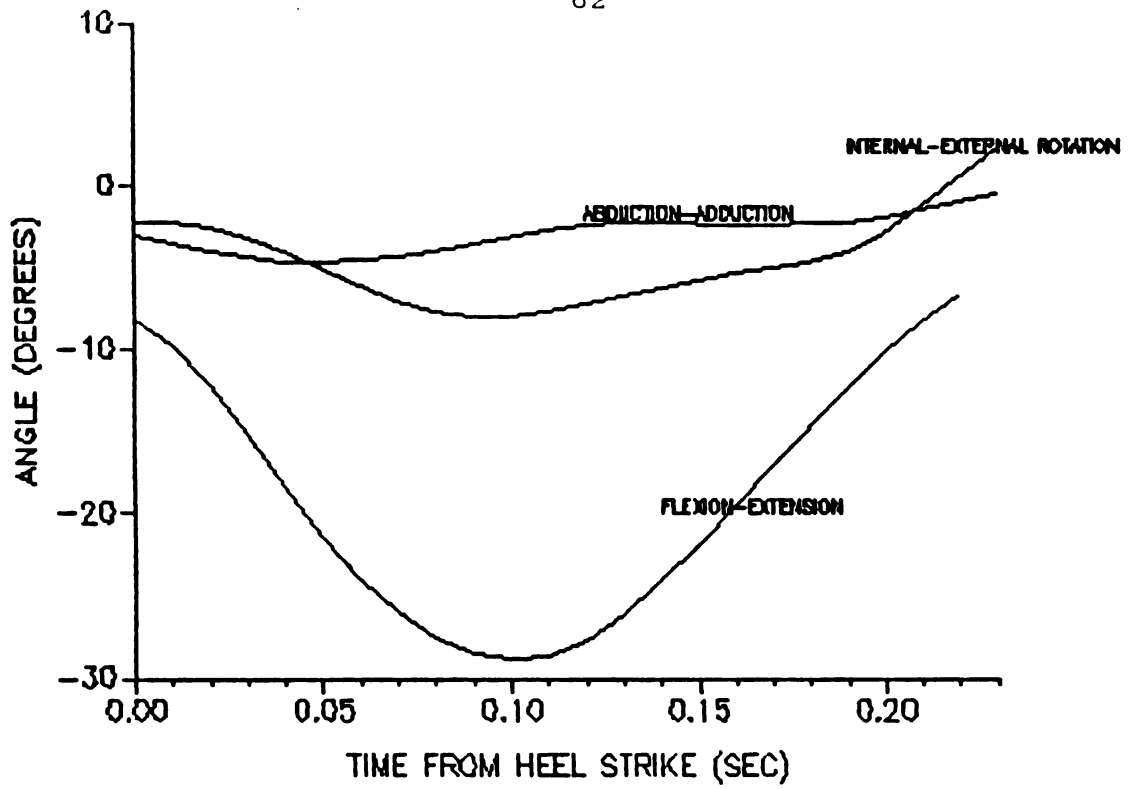


Figure 10. Knee Angles

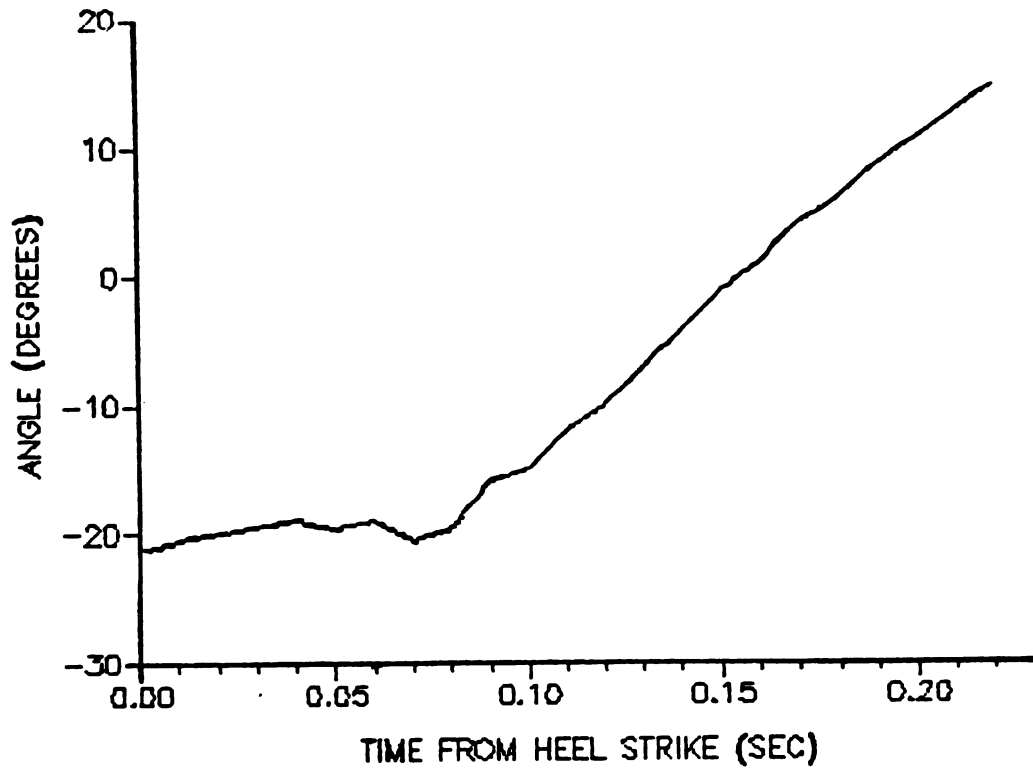


Figure 11. Hip Angles

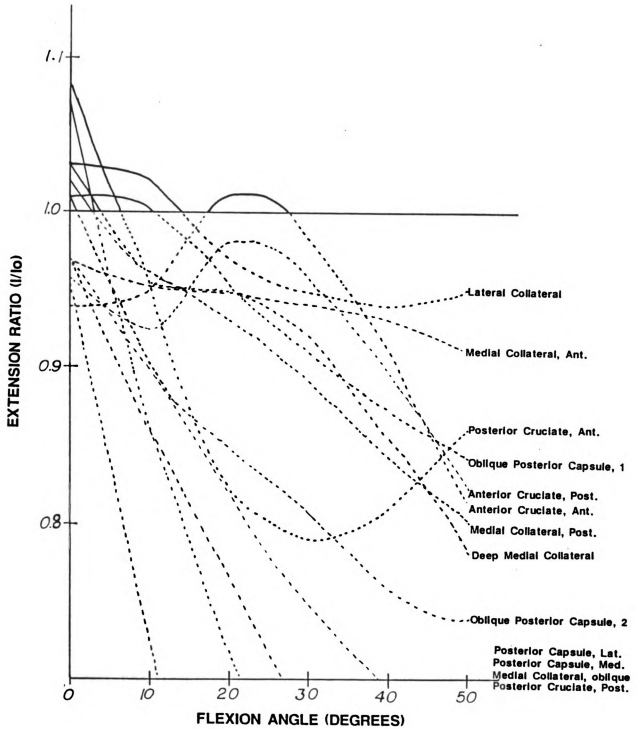


Figure 12. Ligament Extension Ratios with respect to Flexion Angle

ratio becomes less than 1.0, the ligament is considered to be slack and carries no load. For this situation the calculated ligament length is simply the distance between the rotated attachment points.

As can be seen, for most ligaments this model predicts the greatest loading when the limb is near full extension with the structures becoming the most slack between 30° and 50° of flexion. This is in general agreement with experimental observations (27).

The time-varying length patterns during stance phase are shown in Figure 13. For this case, the angles of flexion-extension, abduction-adduction and internal-external rotation discussed earlier were used as the inputs into the model. As would be expected, the greatest calculated lengths are seen near heel strike and toe off, corresponding to the points where the limb is near full extension. The actual moment contributions arising from these ligament deformations were found to be quite small. During midstance where the knee displayed the greatest degree of flexion, this model predicted no load to be carried by the ligamentous components.

From the inputted data the relationships between unknown muscle forces could be developed as outlined in the previous section, resulting in a series of indeterminate problems to be solved by optimization at distinct points in time. Six variations of the problem, using both the simple hinge joint model and the more general model, allowing for a

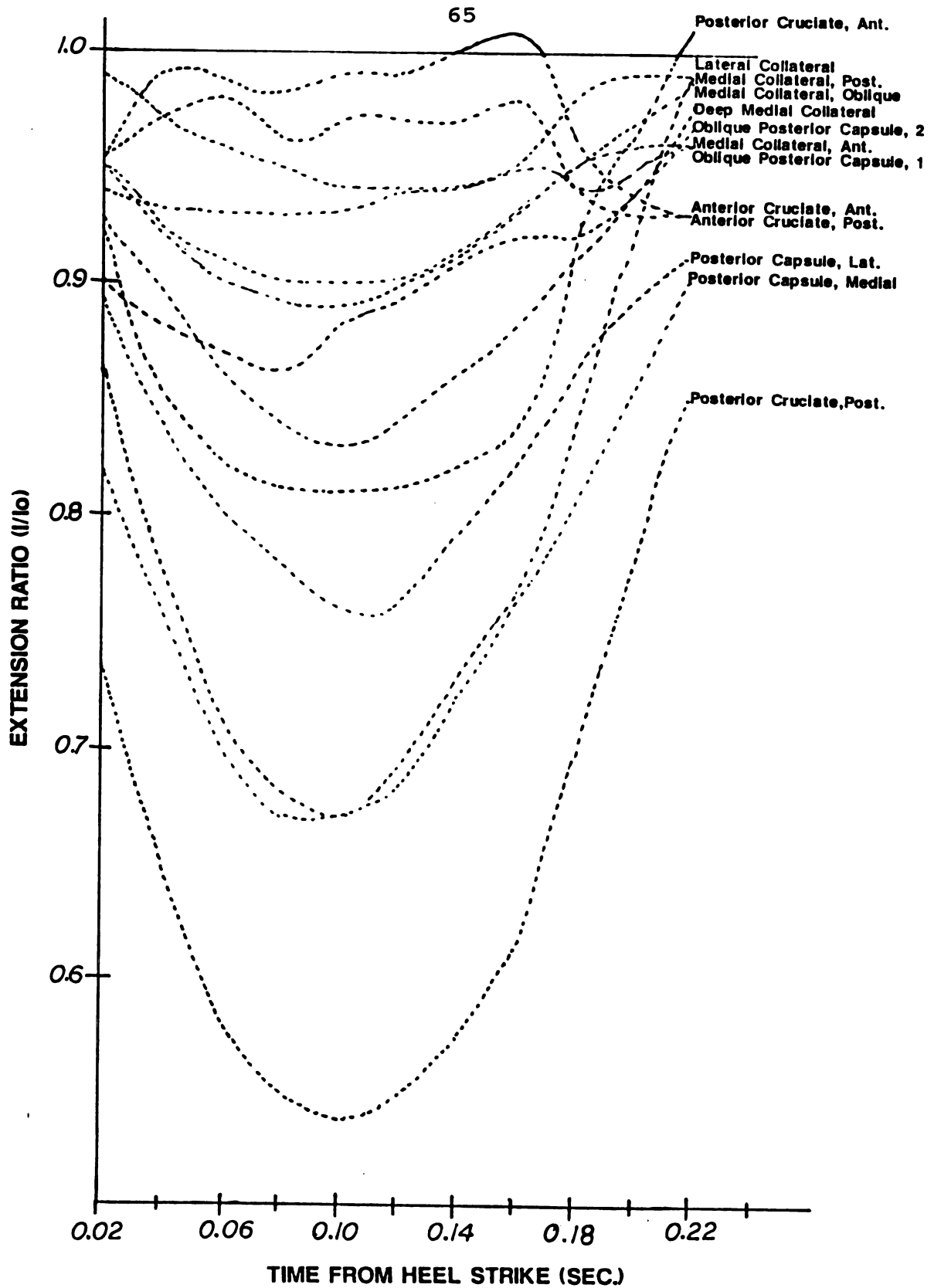


Figure 13. Ligament Extension Ratios, During Stance Phase of Gait

moving contact point, were solved. These corresponded to various methods that have been used in the past to model the knee joint. The cases were:

- I. Three-dimensional model, with moving joint contact and ligamentous contribution
- II. Three-dimensional model, with moving joint contact, no ligamentous contribution
- III. Hinge joint model, no ligaments
- IV. Moving joint contact, muscles satisfy only the flexion-extension moment at knee
- V. Hinge joint model, muscles satisfy only the flexion-extension moment at the knee
- VI. Three-dimensional model, increased tolerances so that muscles are required to satisfy at least 99% of the total joint moment, no ligaments

These six cases resulted in six different sets of time-varying constraints to the optimization problem of minimizing the sum to the muscle stresses cubed. A comparison of the results of these six cases at a point in midstance can be seen in Table 7. No significant ligament force was computed at this time; therefore, the results of Cases I and II, with and without ligaments, are identical. Similarly, Case VI, for which the tolerances on the motion equations were relaxed, shows only minor variation in the calculated muscle forces when compared to the first model. The greatest deviation between the predicted forces is 14.9N which occurs in the patellar ligament. This difference is less than 1% of the total force carried by that structure, though, and is thus quite insignificant.

Table 7. Results For All Six Cases, 0.12 seconds After Heel Strike

MUSCLE	I	II	III	IV	V	VI
Biceps Femoris (long head)	0.0 N					
Gracilis	0.0	0.0	0.0	0.0	0.0	0.0
Rectus Femoris	440.4	440.4	171.2	454.6	453.6	445.6
Sartorius	0.0	0.0	0.0	11.6	10.8	0.0
Semimembranosus	0.0	0.0	0.0	0.0	126.8	0.0
Semitendinosus	51.4	51.4	0.0	20.5	52.4	50.3
Tensor Fasciae Latae	148.3	148.3	180.3	81.2	82.8	145.1
Gastrocnemius (medial)	0.0	0.0	0.0	222.3	0.0	0.0
Gastrocnemius (lateral)	883.7	883.7	1075.9	32.7	0.0	874.8
Biceps Femoris(short)	182.6	182.6	115.9	0.0	0.0	181.9
Vastus Intermedius	466.1	466.1	884.8	404.5	600.8	456.7
Vastus Lateralis	323.5	323.5	615.4	279.7	417.3	318.3
Vastus Medialis	342.5	342.5	651.3	296.1	441.7	336.9
Adductor Brevis 1	0.0	0.0	0.0	0.0	0.0	0.0
Adductor Brevis 2	0.0	0.0	0.0	0.0	0.0	0.0
Adductor Longus	0.0	0.0	0.0	0.4	0.0	0.4
Adductor Magnus 1	0.0	0.0	0.0	0.2	0.0	0.4
Adductor Magnus 2	0.0	0.0	0.0	0.2	0.0	0.3
Adductor Magnus 3	0.0	0.0	0.0	0.1	0.0	0.2
Gluteus Maximus 1	0.0	0.0	0.0	0.0	0.0	0.0
Gluteus Maximus 2	0.0	0.0	0.0	0.2	0.0	0.2
Gluteus Maximus 3	0.0	0.0	0.0	0.6	0.0	0.7
Gluteus Medius 1	483.6	483.6	510.5	522.2	529.8	481.1
Gluteus Medius 2	0.0	0.0	32.7	0.2	25.6	0.0
Gluteus Medius 3	0.0	0.0	0.0	0.0	0.0	0.0
Gluteus Minimus 1	70.7	70.7	71.1	76.5	75.7	70.3
Gluteus Minimus 2	20.7	20.7	39.1	38.1	42.7	17.6
Gluteus Minimus 3	0.0	0.0	0.0	0.0	0.0	0.0
Iliacus	167.7	167.7	159.1	177.5	176.5	167.2
Psoas	31.6	31.6	0.0	4.2	0.0	24.2
Inferior Gemelli	0.0	0.0	0.0	0.0	0.0	0.0
Obturator Externus	0.0	0.0	0.0	0.0	0.0	0.0
Obturator Internus	0.0	0.0	0.0	0.0	0.0	0.0
Pectineus	0.0	0.0	0.0	0.6	0.0	0.3
Piriformis	0.0	0.0	0.0	0.0	0.0	0.0
Quadratus Femoris	0.0	0.0	0.0	0.2	0.0	0.2
Superior Gemelli	0.0	0.0	0.0	0.0	0.0	0.0
Patellar Ligament	1566.8	1566.8	2316.4	1429.7	1906.9	1551.9

The remaining three cases show more pronounced variations. Most notable are the significant increases in the load carried by the three vasti muscles in the simple hinge joint model (III) and the reduction in the predicted force produced by the lateral gastrocnemius for both cases where the muscles are only constrained to satisfy the flexion-extension moment at the knee (IV, V). The former observation is consistent with the idea that posterior movement of the contact point allowed by the more complex model increased the mechanical advantage of the quadriceps muscles. The required moment can thus be produced by a smaller muscle force. The reduction in the gastrocnemius force for cases IV and V indicated that this muscle is being activated primarily to satisfy either the moments of abduction-adduction or internal-external rotation.

The effect of including the ligamentous forces and moments in this model can be seen in Table 8. These results are taken from a point just prior to toe off where the leg is nearly fully extended. As noted previously, at all times during the stance, the ligament contributions are relatively small. For this case the additions of the ligament moments to the motion equations were found to be -0.012 , 0.124 and 0.032 N·m. As can be seen from the predicted muscle force, even this small contribution does have an effect, although it is minor. The largest variation in the predicted forces is 8.5 N.

Table 8. Results, With and Without Ligaments, 0.22 seconds
After Heel Strike

<u>MUSCLE</u>	<u>Ligaments</u>	<u>No Ligaments</u>
Biceps Femoris (long head)	0.3 N	0.0 N
Gracilis	10.0	9.8
Rectus Femoris	138.8	137.8
Sartorius	9.4	9.5
Semimembranosus	213.3	213.8
Semitendinosus	7.9	0.0
Tensor Fasciae Latae	32.4	31.1
Gastronemius (medial)	91.6	89.3
Gastronemius (lateral)	58.0	57.3
Biceps Femoris(short head)	32.3	31.3
Vastus Intermedius	2.0	0.0
Vastus Lateralis	1.2	0.0
Vastus Medialis	1.3	0.0
Adductor Brevis 1	34.2	34.1
Adductor Brevis 2	11.5	11.3
Adductor Longus	153.8	148.9
Adductor Magnus 1	0.0	0.0
Adductor Magnus 2	0.0	0.0
Adductor Magnus 3	0.0	0.0
Gluteus Maximus 1	13.6	13.8
Gluteus Maximus 2	0.0	0.0
Gluteus Maximus 3	0.0	0.0
Gluteus Medius 1	129.7	125.6
Gluteus Medius 2	0.0	0.0
Gluteus Medius 3	0.0	0.0
Gluteus Minimus 1	25.6	25.3
Gluteus Minimus 2	0.0	0.0
Gluteus Minimus 3	0.0	0.0
Iliacus	8.5	0.0
Psoas	103.3	102.8
Inferior Gemelli	0.0	0.0
Obturator Externus	0.0	0.0
Obturator Internus	0.0	0.0
Pectineus	29.3	29.1
Piriformis	0.0	0.0
Quadratus Femoris	0.0	0.0
Superior Gemelli	0.0	0.0
Patellar Ligament	143.3	135.8

The patterns of muscle activity predicted for Cases I, III, IV and V over the complete stance phase are shown in Figures 14 to 27 for selected muscles. All the muscles crossing the knee, with the exception of gracilis and sartorius, which were predicted by this model to carry insignificant loads, are displayed as well as several muscles which cross only the hip. Some general trends can be noted by comparing these results.

Modeling the knee as a simple hinge joint as noted previously caused an increase in activity in the vasti muscles (Figures 22 to 24). This increase is in the magnitude to the forces only, with all cases showing activity only in the first half of the stance phase. On the other hand, the rectus femoris (Figure 15), which with the vasti make up the quadriceps muscle group, shows a decrease in both the magnitude of its peak forces and the time period for which it was active. The lateral gastrocnemius (Figure 20) seems to be minimally affected by this simplification while the medial (Figure 19) displays vastly different patterns for all four cases shown.

The short head of the biceps femoris (Figure 21) shows a decrease in activity with the hinge joint model especially early in the stance. Alternatively, semitendinosus and tensor fasciae latae muscle (Figures 17 and 18) both display much higher peaks while semimembranosus (Figure 16) shows little variation. These latter observations apply only in comparison of the cases where all six motion equations are

applied as constraints. The other two cases display almost identical results for these three muscles, as well as for several others.

Some variations are also seen in the muscles which cross only the hip, such as iliacus (Figure 27) and portions of gluteus medius (Figure 26). Although not directly effected by the choice of knee model, the existence of two joint muscles such as rectus femoris and semimembranosus cause a highly interrelated system to exist and thus differences would be expected.

The effect of enforcing only the flexion-extension moment at the knee is most obvious in the lateral gastrocnemius (Figure 20). A peak force of nearly three times body weight is predicted when the other moments are considered, while almost no activity is seen in this muscle for the case where the muscles are not required to satisfy the moments of abduction-adduction and internal-external rotation. The other head of the gastrocnemius muscle (Figure 19) also displays a vastly different activity pattern. In a comparison of the two cases involving a moving joint center, an extra peak in the force is seen at midstance for the simplified model. A slight reduction in activity is also seen in the three vasti muscles (Figures 22 to 24). As before, this decrease is in magnitude only, not in the time to activity. Rectus femoris, on the other hand, displays little change as a result of this simplification (Figure 15). The peak of activity early in stance for the

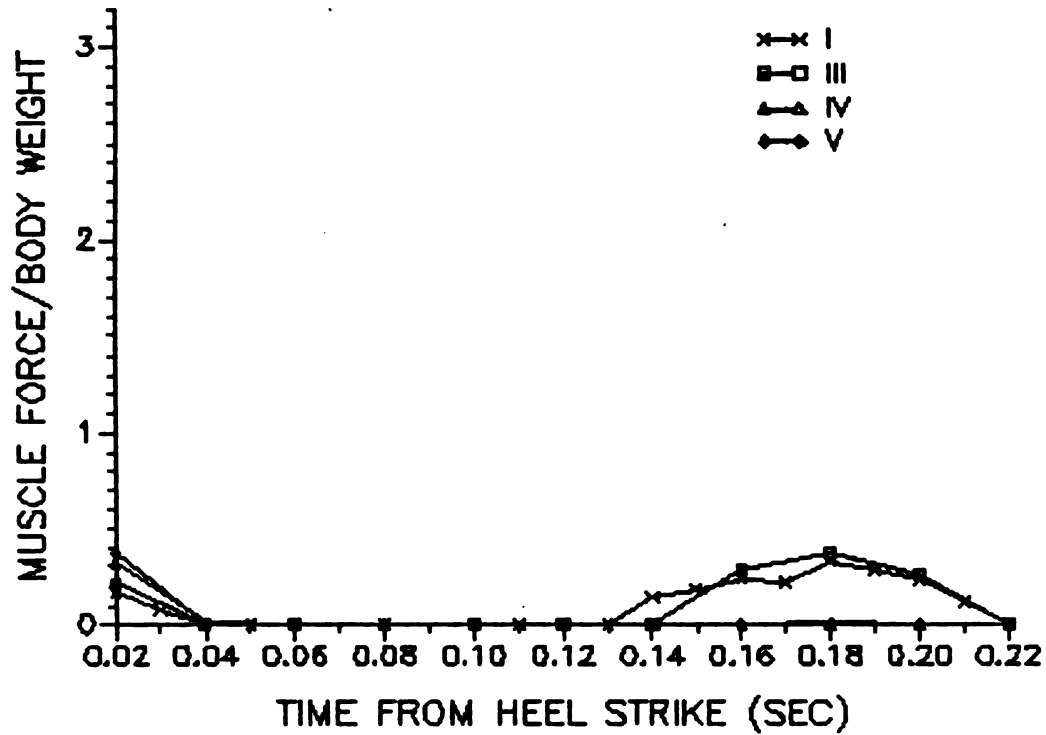


Figure 14. Pattern of Muscle Activity, Long Head of Biceps Femoris

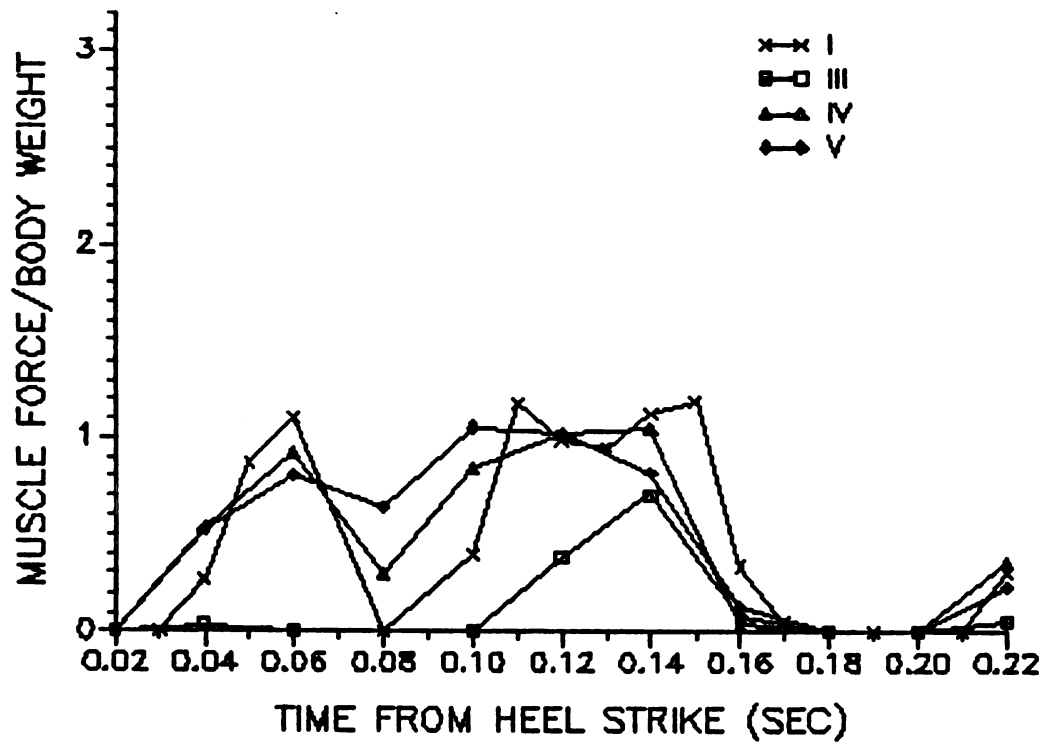


Figure 15. Pattern of Muscle Activity, Rectus Femoris

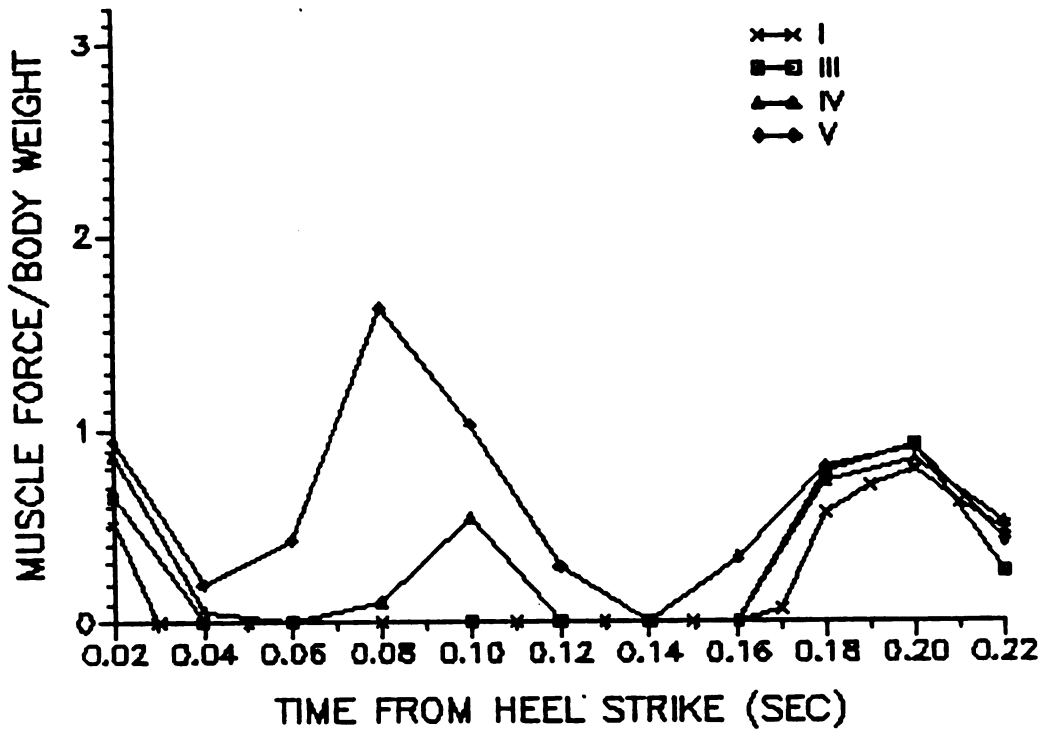


Figure 16. Pattern of Muscle Activity, Semimembranosus

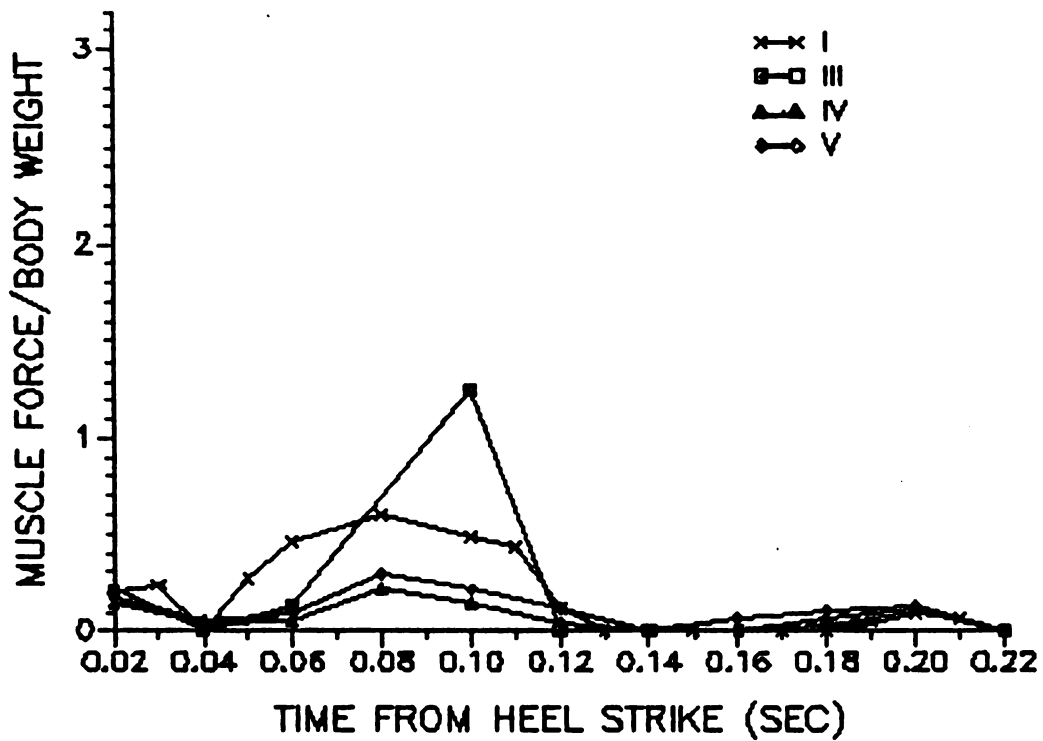


Figure 17. Pattern of Muscle Activity, Semitendinosus

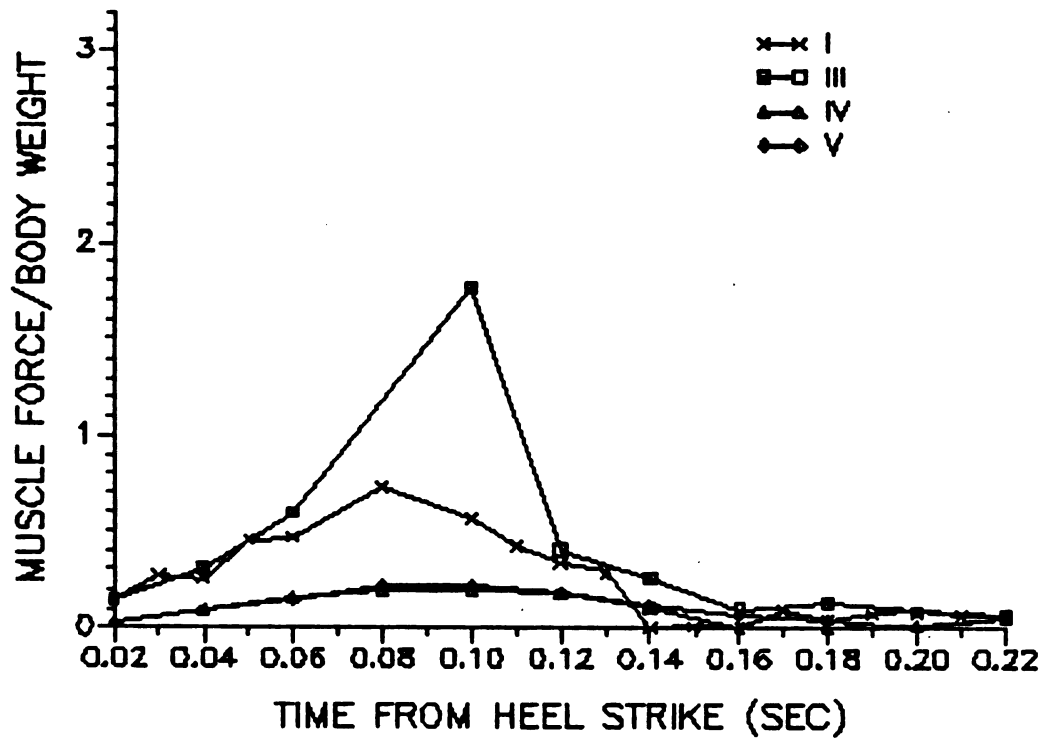


Figure 18 Pattern of Muscle Activity, Tensor Fasciae Latae

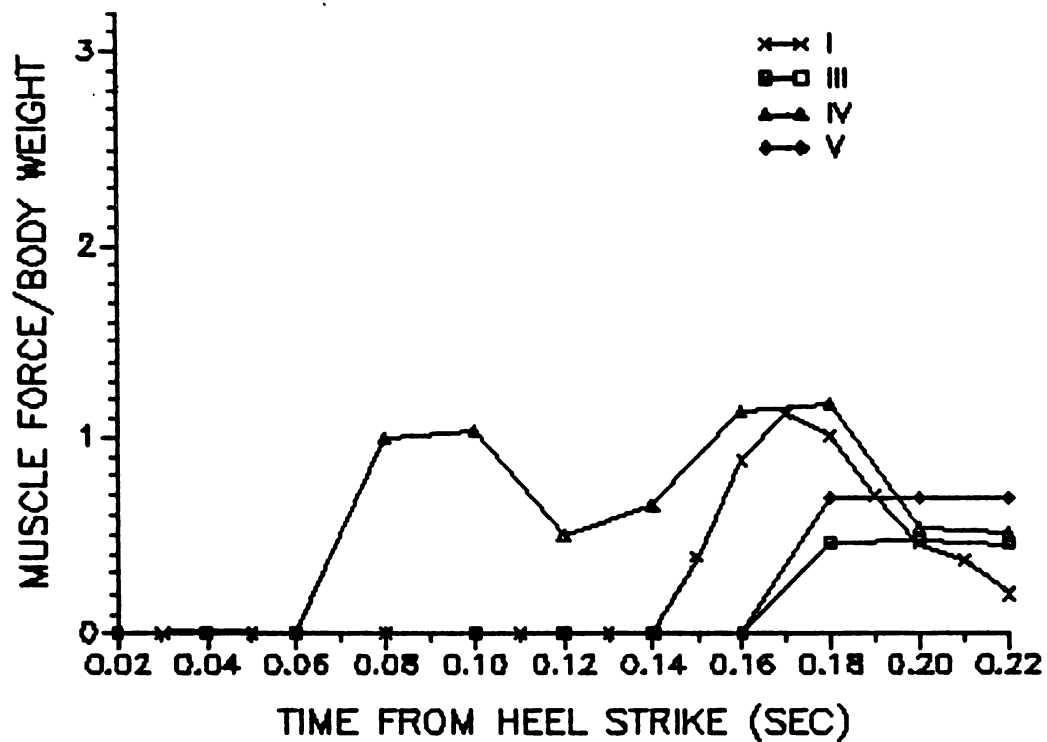


Figure 19. Pattern of Muscle Activity, Medial Gastrocnemius

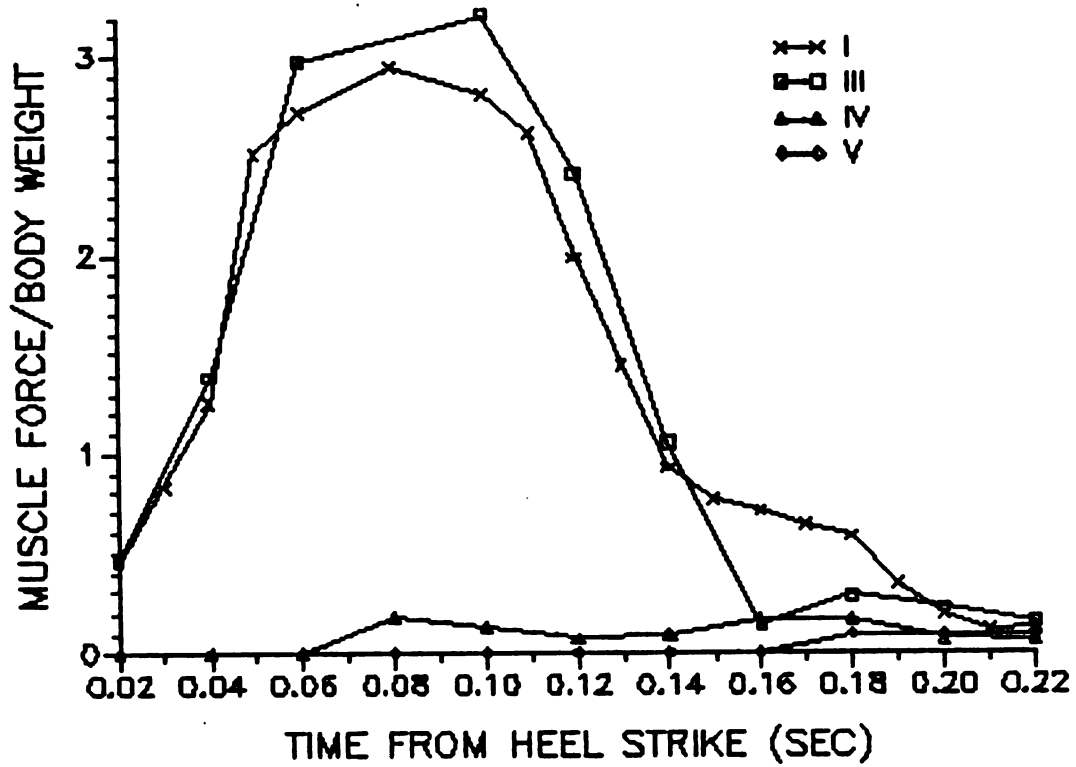


Figure 20. Pattern of Muscle Activity, Lateral Gastrocnemius

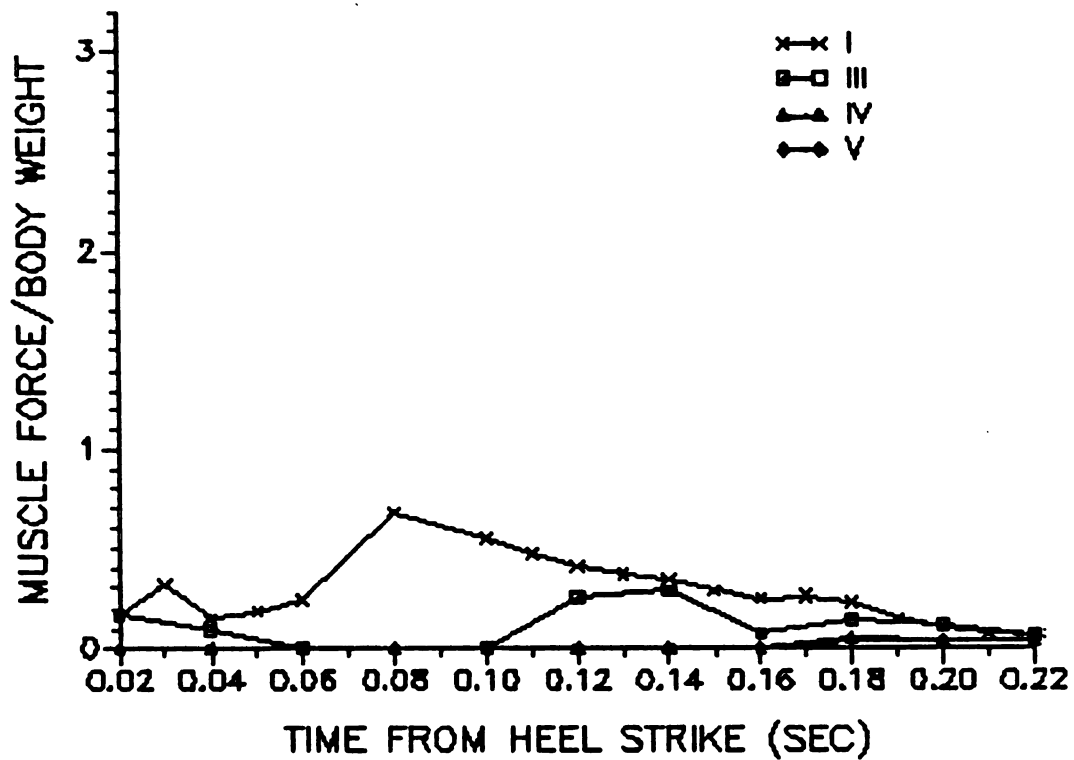


Figure 21. Pattern of Muscle Activity, Short Head of Biceps Femoris

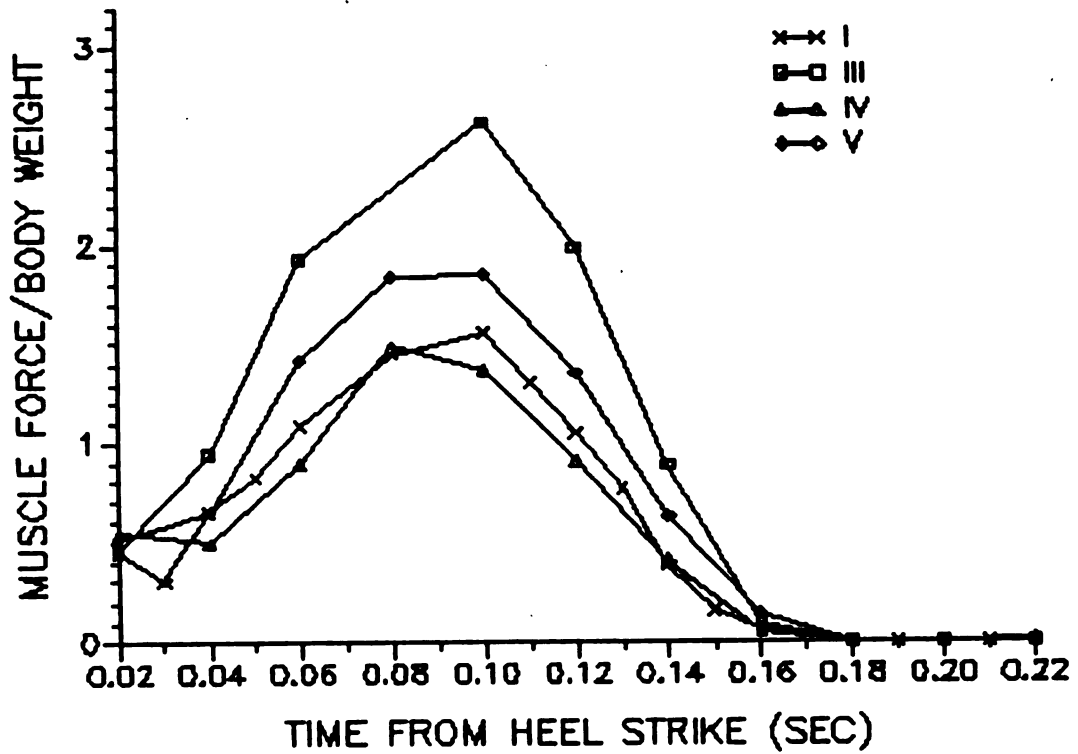


Figure 22. Pattern of Muscle Activity, Vastus Intermedius

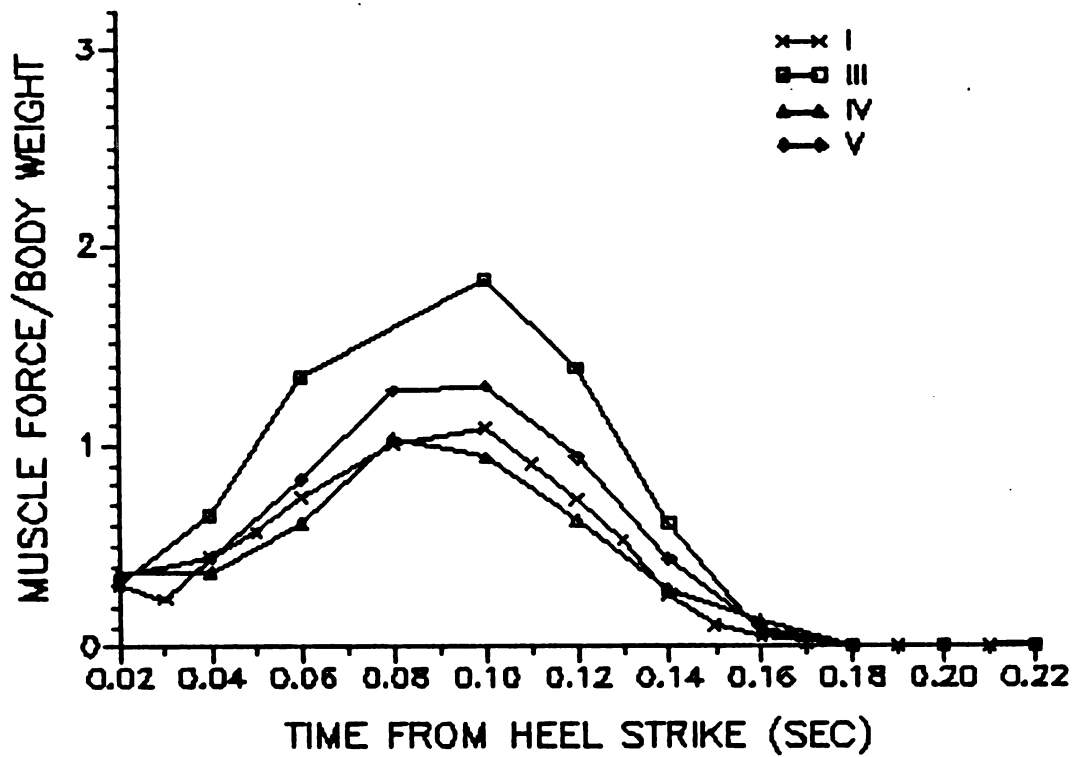


Figure 23. Pattern of Muscle Activity, Vastus Lateralis

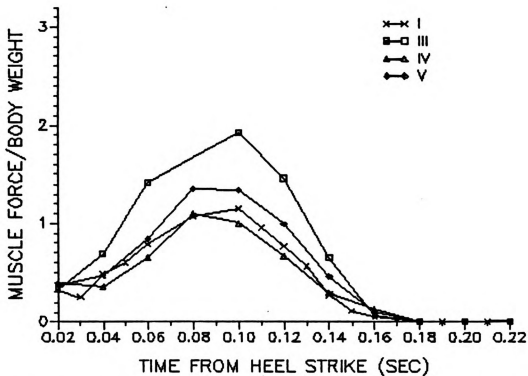


Figure 24. Pattern of Muscle Activity, Vastus Medialis

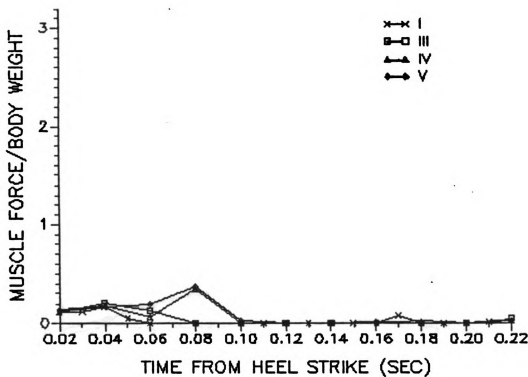


Figure 25. Pattern of Muscle Activity, Gluteus Maximus 1

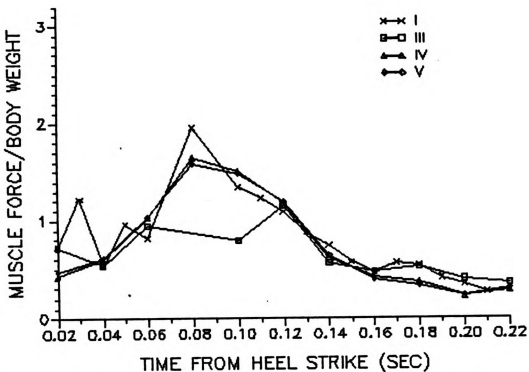


Figure 26. Pattern of Muscle Activity, Gluteus Medius 1

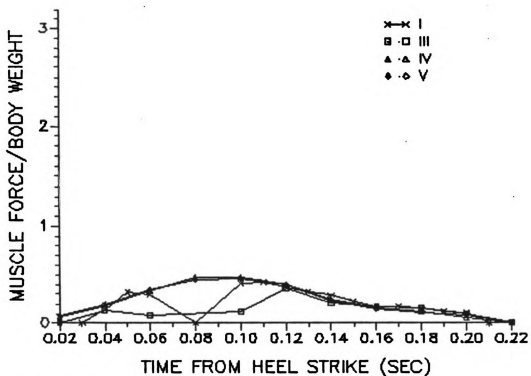


Figure 27. Pattern of Muscle Activity, Iliacus

tensor fasciae latae muscle and semitendinosus (Figures 17 and 18) was greatly decreased for this case while semimembranosus (Figure 16) displayed an extra peak during the same time period.

The limitation of this model, that the muscles are assumed to act along a straight line, is obvious in the time frame immediately following toe off. At that particular point a solution within the feasible set allowed by the constraint equations was not found. When the constraints setting the upper bound of muscle stresses were removed, sartorius was predicted to carry loads corresponding to stresses well over 100 N/cm^2 . Sartorius, a very long thin muscle, curves around the leg, from an origin on the Anterior Superior Iliac Spine to an insertion on the medial side of the tibia, and is in obvious contrast to the straight line representation. Also at this point, the joint contact force drops to an insignificant level due primarily to the lack of a significant ground reaction force to be transferred up the limb. This casts doubts on the validity of the contact condition and thus the relative positions of the tibia and femur at this point.

CONCLUSION

The purpose of this research was to develop a model of muscular, ligamentous and bony structures of the lower limb in order to determine the distribution of the loads that each of these elements carry during various activities. For illustrative purposes, this model was applied to running. The analysis could easily be carried out for any activity for which the necessary kinetic and kinematic data is available.

The model included thirteen ligamentous structures at the knee, 38 muscles crossing the knee and hip and a two-dimensional representation of the contact surfaces at the knee. This latter component of the model provided the capability of modeling the posterior movement of the joint contact. The effects of various simplifications and alternative ways to account for the contributions of the ligaments were also investigated.

For this model the ligament contributions were found to be minimal. Simply increasing the tolerances on the equation of motion constraints developed without the ligaments by 1% and thus requiring the muscles to satisfy only 99% of the moment components at the knee, produced

results which were comparable to the case where the full ligament contribution was included.

The knee is not a simple hinge joint. The complex nature of its motion has been known for years. The results of this investigation show that treating the knee in this simplified manner can greatly affect the results.

The actual criteria used by the body in the selection to muscles is not known. This model assumed an endurance based criteria, but others have been suggested, including a random selection process. In reality, the body may use a combination of these types of criteria or some other criteria that has not even been considered. Verification of the results is difficult. Comparison to EMG data can only be done temporally. Other investigators have demonstrated that times of muscle activity vary depending on the optimization criteria selected (30). This research has shown that these times are model sensitive as well.

Even in the more complete models included in this study, many simplifications were made which could have major consequences in the results. Future investigation may focus on improving the validity of the model. The three-dimensional nature of the muscle model allowed for the prediction of synergistic and antagonistic functions of the various muscles. The two dimensional representation of joint surfaces and the assumption of a single point of joint contact, though, present possible sources of error. This model treats the problem in a quasi-static way and the

dynamic process is treated as a series of independent problems at discrete time intervals. It is encouraging to note, though, that the results show relatively smooth curves over the time interval studied.

While the ligaments were treated as strictly structural components, mechano-receptors are known to exist within the ligaments of the knee. In recent years, the role of these elements as part of a complex neuromuscular feedback mechanism has been the subject of an increasing amount of study. The effect of this alternative role, especially in light of the relatively insignificant structural contribution found in this model, is definitely worthy of further investigation.

The results of this study have benefits to physicians, therapists and others needing to understand the role played by muscles and other internal structures. Even with the modeling compromises made, this work gives insight into the functioning of the human body. It shows which muscles can provide the various moment components and offers a possible solution.

APPENDIX

APPENDIX

GENERALIZED REDUCED GRADIENT METHOD

In basic calculus, a function of one variable has a local internal minimum at the point where its first derivative is zero and its second derivative is positive. For the general unconstrained n-dimensional optimization problem this idea translates into the requirements that for a point to be a local minimum the gradient of the objective function must be zero ($\nabla F(X) = 0$) and the matrix of second partial derivatives of the function with respect to the design variables must be positive definite. This matrix is known as the Hessian matrix and positive definiteness means that it has all positive eigenvalues.

The constrained nonlinear problem presents additional difficulties since the design must also remain within the feasible set. This can present a case analogous to the single variable situation where the minimum is located at an endpoint of the interval for which the function is defined.

The basic constrained optimization problem can be written mathematically as:

$$\begin{array}{lll} \text{minimize} & F(X) & X \in R^n \\ \text{(A1) subject to} & h_k(X) = 0 & k = 1,1 \\ & g_j(X) \leq 0 & j = 1,m \\ & X_i^L \leq X_i \leq X_i^U & i = 1,n \end{array}$$

The conditions necessary for a given point to be a minimum for this problem are that:

$$(A2) \quad \nabla F(x^*) + \sum \lambda_i \nabla g_i(x^*) + \sum \mu_j \nabla h_j(x^*) = 0$$

and $\lambda_i g_i(x^*) = 0$

$$\lambda_i \geq 0$$

These are known as the Kuhn-Tucker Conditions.

The generalized reduced gradient method of nonlinear programming is one algorithm that can be used to locate a design which satisfies these conditions. The following description of this method was referenced from Garret N. Vanderplaats (38).

The aforementioned problem can be simplified to one involving only equality and side constraints by the introduction of non-negative slack variables for each of the m inequality constraints. The resulting problem has a total of $m + n$ design variables and is of the form:

$$(A3) \quad \begin{array}{lll} \text{minimize} & F(X) & X \in R^{n+m} \\ \text{subject to} & h_k(X) = 0 & k = 1,1 \\ & g_j(X) + X_{j+n} = 0 & j = 1,m \\ & X_i^L \leq X_i \leq X_i^U & i = 1,n \\ & X_{j+n} \geq 0 & j = 1,m \end{array}$$

By assuming that the upper bounds associated with the slack variables are set very large, i.e. infinite, and the lower

bound for each is zero, the problem can be further generalized to:

$$\begin{array}{lll}
 \text{minimize} & F(X) & X \in R^{n+m} \\
 \text{(A4) subject to} & h_j(X) = 0 & j = 1, m+1 \\
 & X_i^L \leq X_i \leq X_i^U & i = 1, n+m
 \end{array}$$

The basic concept of the generalized reduced gradient method is to recognize that for each equality constraint a dependent design variable can be defined, thereby reducing the total number of independent design variables. The vector representation of the design, X , can be partitioned into:

$$(A5) \quad X = (Z, Y)^T$$

where: Z = the $n-1$ independent design variables

Y = the $m+1$ dependent design variables

Note that there are no restrictions as to which variables are contained in Z and which are in Y . Now the objective becomes:

$$(A6) \quad F(X) = F(Z, Y)$$

To improve a given design, a direction vector must be determined which will reduce the objective without violating any constraints. From equations A3 a generalized reduced gradient, G_R , can be found. This vector is used to define a search direction, S , for use in the iterative process defined by:

$$(A7) \quad X_i^q = X_i^{q-1} + \alpha^* S^q$$

where: q = the iteration number

S = the vector search direction

α^* = the step size

At each iteration the value of α^* which gives the minimum value of the objective, $F(X)$ is found and used to define the new value of X . This involves a one-dimensional optimization along the search direction, S .

In its simplest form, the search direction is defined by:

$$(A8) \quad \vec{S} = -\vec{G}_R$$

In order to maintain movement in a feasible direction, i.e. to prevent violation of the side constraints, this relationship is modified slightly so that:

$$(A9) \quad S_i = \begin{cases} -r_i & \text{if } z_i^L < z_i < z_i^U \text{ or } r_i > 0 \\ 0 & \text{otherwise} \end{cases}$$

where S_i and r_i are the individual components of S and G_R respectively.

The algorithm for calculating G_R for the general nonlinear case can best be understood by first considering the situation where $h_j(X) = 0$ is a linear system of equations and can be represented by:

$$(A10) \quad \tilde{A} X = b$$

If X is partitioned into dependent and independent variables as outlined above this expression becomes:

$$(A11) \quad \tilde{B} Y + \tilde{C} Z = b$$

and the dependent variables, Y , can be found by:

$$(A12) \quad Y = \tilde{B}^{-1} (b - \tilde{C} Z)$$

The objective function can then be represented by:

$$(A13) \quad f(Z) = F(Z, Y) = F(\tilde{B}^{-1}(b - \tilde{C} Z), Z)$$

and by the chain rule:

$$(A14) \quad \nabla_Z f = \nabla_Z F + \nabla_Y F \nabla_Z Y$$

But $\nabla_Z Y = -\tilde{B}^{-1} \tilde{C}$, therefore:

$$(A15) \quad \nabla_Z f = \nabla_Z F - \tilde{B}^{-1} \tilde{C} \nabla_Y F$$

This defines the generalized reduced gradient, G_R , which can be viewed as $\nabla F(X)$ of the unconstrained function, $f(Z)$. To extend this analysis to the nonlinear case an imaginary hyper-plane, $H(X) = 0$, tangent to the constraint $h(X) = 0$ at the initial design X_0 , is defined by:

$$(A16) \quad H(X) = h(X_0) + \nabla_X h (X - X_0)$$

If X_0 is feasible, $h(X_0) = 0$. For some point near X_0 , say $X = (Z, Y)^T$ to be feasible, $h(Y, Z)$ must be equal to zero as well. Assuming that $h(Y, Z) \approx 0$, or in other words $H(X) = 0$, is satisfactory, equation A16 becomes:

$$(A17) \quad \nabla_X h (X - X_0) = 0$$

With $\nabla_X h$ a constant for each iteration, this relationship is equivalent to $\tilde{A} X = b$ of before. Thus $\nabla_Y h$ and $\nabla_Z h$ correspond to \tilde{B} and \tilde{C} and $Y = Y_0 - \nabla_Y h^{-1} \nabla_Z h (Z - Z_0)$.

Then as before:

$$(A18) \quad \nabla_Z f = \nabla_Z F - \nabla_Y F [\nabla_Y h]^{-1} [\nabla_Z h]$$

This relationship applies for suitably small values of α .

For larger step sizes the difference between the values of

$H(X)$ and $h(X)$ becomes significant. During various

iterations the dependent variables, Y , must be updated.

However, since $H(X)$ is simply a linear approximation to the

original nonlinear problem, the constraints may not be satisfied for a specific α . A new expression for dY must then be developed in order to drive $h(X)$ to zero. This corresponds to Newton's method for solving simultaneous nonlinear equations.

BIBLIOGRAPHY

BIBLIOGRAPHY

1. An, K.N., B.M. Kwak, E.Y. Chao, B.F. Morrey, "Determination of Muscle and Joint Forces: A New Technique to Solve the Indeterminate Problem," Journal of Biomechanical Engineering, Vol. 106, No. 4, pp. 364-367, 1984.
2. Andriacchi, T.P., R.P. Mikosz, S.J. Hampton, J.O. Galante, "Model Studies of the Stiffness Characteristics of the Human Knee Joint," Journal of Biomechanics, Vol. 16, No. 1, pp 23-29, 1983.
3. Barbenel, J.L., " The Biomechanics of the Temporomandibular Joint: A Theoretical Study," Journal of Biomechanics, Vol. 5, pp. 251-256, 1972.
4. Bean, J.C., D.B. Chaffin, A.B. Schultz, "Biomechanics Model Calculations of Muscle Contractions Forces: A Double Linear Programming Method," Journal of Biomechanics, Vol. 21, No. 1, pp. 59-66, 1988.
5. Brand, R.A., R.D. Crowninshield, C.E. Wittstock, D.R. Pedersen, C.R. Clark, F.M. vanKrieken, "A Model of Lower Extremity Muscular Anatomy," Journal of Biomechanical Engineering, Vol 104, pp. 304-310, 1982.
6. Brand, R.A., D.R. Pedersen, J.A. Of, "The Sensitivity of Muscle Force Predictions to Changes in Physiological Cross-Sectional Area," Journal of Biomechanics, Vol. 19, No. 8, pp. 589-596, 1986.
7. Bresler, E., J.B. Frankel, "The Forces and Moments in the Leg During Walking," Journal of Applied Mechanics, Vol. 72, pp. 27-36, 1950.
8. Buff, H.U., L.C. Jones, D.S. Hungerford, "Experimental Determination of Forces Transmitted Through the Patello-Femoral Joint," Journal of Biomechanics, Vol. 21, No. 1, pp.17-23, 1988.
9. Crowninshield, R.D., "Use of Optimization Techniques to Predict Muscle Forces," Journal of Biomechanical Engineering, Vol. 100, pp. 88-92, 1978.

10. Crowninshield, R.D., R.A. Brand, "A Physiologically Based Criterion of Muscle Force Prediction in Locomotion," Journal of Biomechanics, Vol. 14, No. 11, pp. 793-801, 1981.
11. Crowninshield, R.D., M.H. Pope, R.J. Johnson, "An Analytical Model of the Knee," Journal of Biomechanics, Vol. 9, pp. 397-405, 1976.
12. Davy, D.T., M.L. Audo, "A Dynamic Optimization Technique for Predicting Muscle Forces in the Swing Phase of Gait," Journal of Biomechanics, Vol 20, No. 2, pp. 187-201, 1987.
13. Dul, J., G.E Johnson, R. Shiavi, M.A. Townsend, "Muscular Synergism - II. A Minimum-Fatigue Criterion for Load Sharing Between Synergistic Muscles," Journal of Biomechanics, Vol. 17, No. 9, pp. 675-684, 1984.
14. Elftman, H., "Forces and Energy Changes in the Leg During Walking," American Journal of Physiology, Vol 125, pp. 339-356, 1939.
15. Ellis, M.I., B.B. Seedhom, V. Wright, D. Dowson, "An Evaluation of the Ratio Between the Tensions Along the Quadriceps Tendon and the Patellar Ligament," Engineering in Medicine, Vol. 9, No. 4, pp. 189-194, 1980.
16. Gracovetsky, S., H.F. Farfan, C. Lamy, "A Mathematical Model of the Lumbar Spine Using an Optimized System to Control Muscles and Ligaments," Orthopedic Clinics of North America, Vol. 8, No. 1, pp. 135-153, 1977.
17. Grood, E.S., M.S. Hefzy, "An Analytical Technique for Modeling Knee Joint Stiffness - Part I: Ligamentous Forces," Journal of Biomechanical Engineering, Vol. 104, pp. 330-337, 1982.
18. Grood, E.S., W.J. Suntay, "A Joint Coordinate System for the Clinical Description of Three-Dimensional Motions: Applications to the Knee," Journal of Biomechanical Engineering, Vol 105, pp. 136-144, 1983.
19. Hardt, D.E., "Determining Muscle Forces in the Leg During Normal Human Walking - An Application and Evaluation of Optimization Methods," Journal of Biomechanical Engineering, Vol. 100, pp. 72-78, 1978.
20. Hefzy, M.S., E.S. Grood, "Review of Knee Models," Applied Mechanical Reviews, Vol. 41, No. 1, 1988.

21. Hefzy, M.S., E.S. Groom, "An Analytical Technique for Modeling Knee Joint Stiffness - Part II: Ligamentous Geometric Nonlinearities," Journal of Biomechanical Engineering, Vol. 105, pp. 145-153, 1983.
22. Iseki, F., T. Tomatsu, "The Biomechanics of the Knee Joint with Special Reference to the Contact Area," Keio Journal of Medicine, Vol. 25, pp. 37-44, 1976.
23. Lew, W.D., J.L. Lewis, "An Anthropometric Scaling Method with Application to the Knee Joint," Journal of Biomechanics, Vol. 10, pp. 171-181, 1977.
24. Lew, W.D., J.L. Lewis, "A Technique for Calculating in Vivo Ligament Lengths with Application to the Human Knee Joint," Journal of Biomechanics, Vol. 11, pp. 365-377, 1978.
25. MacConaill, M.A., "The Ergonomic Aspects of Articular Mechanics," Studies on the Anatomy and Function of Bones and Joints, pp. 69-80, Springer, Berlin, 1967.
26. Mikosz, R.P., T.P. Andriacchi, G.B.J. Andersson, "Model Analysis of Factors Influencing the Prediction of Muscle Forces at the Knee," Journal of Orthopaedic Research, Vol. 6, pp. 205-214, 1988.
27. Moeinzadeh, M.H., A.E. Engin, N. Akkas, "Two-Dimensional Dynamic Modeling of Human Knee Joint," Journal of Biomechanics, Vol. 16, No. 4, pp. 253-264, 1983.
28. Morrison, J.B., "Bioengineering Analysis of Force Actions Transmitted by the Knee Joint," Bio-Medical Engineering, Vol. 3, pp. 164-170, 1968.
29. Patriarco, A.G., R.W. Mann, S.R. Simon, J.M. Mansour, "An Evaluation of the Approaches of Optimization Models in the Prediction of Muscle Forces During Human Gait," Journal of Biomechanics, Vol. 14, No. 8, pp. 513-525, 1981.
30. Pedersen, D.R., R.A. Brand, C. Cheng, J.S. Arora, "Direct Comparison of Muscle Force Predictions Using Linear and Nonlinear Programming," Journal of Biomechanical Engineering, Vol. 109, pp. 192-199, 1987.
31. Pedersen, D.R., R.A. Brand, "Three-Dimensional Modeling of the Pelvic Limb," 1987, Unpublished.
32. Pedotti, A., V.V. Krishnan, L. Stark, "Optimization of Muscle-Force Sequencing in Human Locomotion," Mathematical Biosciences, Vol. 38, pp. 57-76, 1978.

33. Penrod, D.D., Davy, D.T., Singh, D.P., "An Optimization Approach to Tendon Force Analysis," Journal of Biomechanics, Vol. 7, pp. 121-129, 1974.
34. Seireg, A., R.J. Arvikar, "The Prediction of Muscular Loads Sharing and Joint Forces in the Lower Extremities During Walking," Journal of Biomechanics, Vol. 8, pp. 89-102, 1975.
35. Seireg, A., R.J. Arvikar, "A Mathematical Model for Evaluation of Forces in Lower Extremities of the Musculo-Skeletal System," Journal of Biomechanics, Vol. 6, pp. 313-326, 1973.
36. Soderburg, G.L., W.F. Dostal, "An Electromyographic Study of Three Parts of the Gluteus Medius During Activities of Daily Living," Journal of the American Physical Therapy Association, Vol. 58, pp. 691-696, 1978.
37. Strasser, H., Lehrbuch der Muskel und Gelenkmechanik, Springer, Berlin, Vol. 3, 1917.
38. Vanderplaats, G.N., Numerical Optimization Techniques for Engineering Design; with Application, McGraw-Hill Book Company, 1984.
39. Yeo, B.P., "Investigations Concerning the Principle of Minimal Total Muscular Force," Journal of Biomechanics, Vol. 9, pp. 413-416, 1976.
40. Weber, W., E. Weber, Mechanik der Menschlichen Gehrwerkzeuge (Mechanics of Human Locomotion), Gottingen, pp. 161-202, 1836.
41. Wismans, J., F. Veldpaus, J. Janssen, A. Huson, P. Struben, "A Three-Dimensional Mathematical Model of the Knee Joint," Journal of Biomechanics, Vol 13, pp.677-685, 1980.
42. Zajac, F.E., R.W. Wicke, W. S. Levine, "Dependence of Jumping Performance of Muscle Properties When Humans Use Only Calf Muscles for Propulsion," Journal of Biomechanics, Vol. 17, No. 7, pp. 513-523, 1984.